

Impact Hamiltonian systems and polygonal billiards

L. Becker, S. Elliott, B. Firester, S. Gonen Cohen, M. Pnueli, V. Rom-Kedar¹,

Department of Computer Science and Applied Mathematics,

The Weizmann Institute of Science, Rehovot, Israel

¹The Estrin Family Chair of Computer Science and Applied Mathematics.

December 21, 2024

Abstract The dynamics of a beam held on a horizontal frame by springs and bouncing off a step is described by a separable two degrees of freedom Hamiltonian system with impacts that respect, point wise, the separability symmetry. The energy in each degree of freedom is preserved, and the motion along each level set is conjugated, via action angle coordinates, to a geodesic flow on a flat two-dimensional surface in the four dimensional phase space. Yet, for a range of energies, these surfaces are not the simple Liouville-Arnold tori - these are tori of genus two, thus the motion on them is not conjugated to simple rotations. Namely, even though energy is not transferred between the two degrees of freedom, the impact system is quasi-integrable and is not of the Liouville-Arnold type. In fact, for each level set in this range, the motion is conjugated to the well studied and highly non-trivial dynamics of directional motion in L-shaped billiards, where the billiard area and shape as well as the direction of motion vary continuously on iso-energetic level sets. Return maps to Poincaré section of the flow are shown to be conjugated, on each level set, to interval exchange maps which are computed, up to quadratures, in the general nonlinear case and explicitly for the case of two linear oscillators bouncing off a step. It is established that for any such oscillator-step system there exist step locations for which some of the level sets exhibit motion which is neither periodic nor ergodic. Changing the impact surface by introducing additional steps, staircases, strips and blocks from which the particle is reflected, leads to iso-energy surfaces that are foliated by families of genus k level set surfaces, where the number and order of families of genus k depend on the energy.

1 Introduction

Quasi-integrable dynamics appears in non-convex billiards with boundary consisting of horizontal and vertical segments [26, 27, 2] and in non-convex billiards created by segments belonging to confocal quadrics [6, 7, 11]. The resulting dynamics are related to deep mathematical theories on Interval Exchange Maps (IEM), on directed motion on translation surfaces, on genericity of curves in the space of affine lattices, on the Teichmüller geometry of moduli space and even on some results in Number theory (see [4, 11, 23] and references therein). We show that this fascinating collection of inter-related mathematical fields are also related to the rich research area of Hamiltonian Impact Systems (HIS). Thus, these theories are related to a large variety of physically realizable models. We present this connection in the simplest possible setting and in the discussion we comment on some future synergetic directions.

In [26, 6] the two known integrable billiards in the plane, rectangles and ellipses, are modified by considering non-convex boundaries consisting of segments that respect the symmetries of the integrable billiard dynamics. The resulting tables, *nibbled rectangles* [2]- domains defined by segments of horizontal and vertical boundaries (the simplest non-trivial geometries are slitted rectangle and L-shaped billiards, see, e.g. Fig 2) and *nibbled ellipses* [6, 7, 11, 10] - domains defined by segments of confocal quadrics, display fascinating dynamical properties. The nibbled rectangles are rational polygons and are thus analyzed by constructing, by reflections along the horizontal and vertical segments, a flat surface (possibly with singularities). Then, the directional billiard flow on the nibbled rectangle is conjugated to the geodesic flow on the glued flat surface. The genus of the flat surface is computable depending only on the number and type of corners (see [2] and references therein). The return map to a transverse section of the surface is an IEM, and thus, the dynamics on the flat surface and the properties of the IEM are related. The dynamics on a given surface depend on the direction of motion. For a flat torus, the dynamics satisfy the Veech dichotomy: depending on the direction, either the motion is periodic or uniquely ergodic. The higher genus surfaces that are produced by the nibbled rectangles do not necessarily satisfy this condition; For the tables that do not produce lattice surfaces, there can be directions of motion for which the dynamics are uniquely ergodic, directions of motion such that a band of periodic trajectories co-exists with a band of trajectories that are dense on some set in the associated flat surface, and there can be also directions which are ergodic but not uniquely ergodic. Characterizing the measure of these sets of directions for a given billiard, the measure of parameters on which such behavior occurs for a given family of billiards, and defining proper statistical properties of the dynamics for such directions are delicate problems which are under current study, see e.g. [4, 2, 22, 14, 11, 10] and references therein.

In [6, 7, 11, 10] it was discovered that the above tools may be applied to the study of the

dynamics in nibbled ellipses. Since reflections from confocal quadrics preserve the same integral of motion, for any fixed integral of motion a conjugacy to a directional motion on a glued flat surface is found, and, thus, an IEM can be constructed. Notably, each constant of motion (namely, each caustic) in a nibbled elliptic table defines a directional flow on a different flat surface while the direction of motion is fixed [11]. Recently it was established that under some conditions on the nibbled ellipse the family of directional flow on the resulting surfaces corresponds to a generic curve in the corresponding moduli space [11, 10]. We show here that a rich class of HIS produces families of directional flow on flat surfaces, where both the direction and the geometry of the surfaces vary piecewise smoothly. While the question of conditions for genericity of the flow on iso-energetic surfaces remains open, the tools developed in [11, 10] appear relevant.

The field of Hamiltonian Impact Systems (HIS), which corresponds to a smooth conservative motion in a domain with elastic impacts from its boundaries, combines two types of dynamical systems - the non-trivial, possibly chaotic, smooth motion associated with Hamiltonian flows [1], and, the dynamics resulting from elastic impacts, which have been extensively studied mainly in the context of billiards [17]. The combination of these two fields is natural from a modeling point of view, as, in many systems, there is a smooth bounded interaction component (e.g. attraction between atoms) and short range repulsion (e.g. atomic repulsion between atoms) giving rise to steep potentials that may be approximated, as a singular perturbation, by elastic reflections [17, 18, 15, 19]. Analysis of non-integrable HIS includes local analysis near periodic orbits of the HIS [8, 15, 3], analysis near homoclinic orbits of the HIS [18], studies of the impact dynamics in some adiabatic limits [13, 12], persistence of KAM tori of motion along convex boundaries [25], and even establishment of hyperbolic behavior for some specific type of systems of particles [24].

Recently, a new class of HIS systems which is amenable to analysis under various perturbation was defined - the Integrable Hamiltonian Impact Systems (IHIS) - these are integrable Hamiltonian systems with impact surfaces which respect the integrability symmetries [19]. The main examples for such systems are mechanical separable Hamiltonians (i.e. $H(q, p) = \sum_{i=1}^N (\frac{p_i^2}{2m} + V(q_i))$), where the impact surface is a wall in the configuration space with a normal aligned along one of the q_i axis (the extension of these ideas to HIS with quadratic potentials in elliptic billiards [9, 21] is under current study). Then, impacts simply send $p_i \rightarrow -p_i$ and do not destroy the separability of the system. If the walls are infinite the symmetry of the separable dynamics is preserved and the resulting dynamics of the IHIS are Liouville integrable [19]. The class of IHIS enriches the number of integrable impact systems from merely two families for billiards (ellipsoidal billiards [5] and rectangles) to the huge class of all integrable Hamiltonian systems with the properly defined impact surfaces. In [19] we establish KAM type results for perturbations of IHIS away from its tangent singularities. Here, the appearance of Quasi-Integrable HIS (QIHIS) is explored by introducing impact surfaces that are composed of finite or semi-infinite segments that respect the

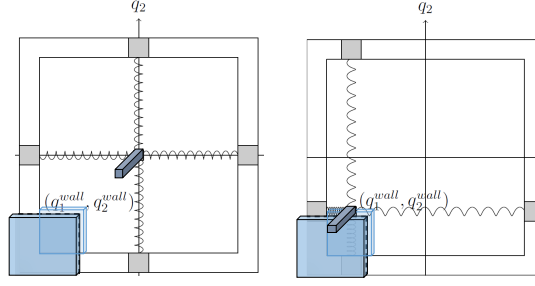


Figure 1: A mechanical model for the Hamiltonian-step system (Eqs. (1) and (3)). (a) A rigid beam is confined between rigid horizontal and vertical springs hinged to supports that slide with no friction along a frame. (b) Two aligned rigid steps are placed in front and on the back of the frame, so when the beam hits these barriers an elastic impact occurs.

symmetries of the integrable dynamics.

To simplify the presentation we consider one of the simplest possible QIHIS: two uncoupled oscillators that impact from a single right step in the configuration space, see Figure 1 for a physical realization of such a system; A springy beam is held on a horizontal frame and reflects from a step. The springs are connected to slider blocks that slide with no friction along a rectangular frame of ducts, and the step-walls, marked by a dotted line are out of the frame plane so that the slider blocks slide freely under the step walls and do not collide with them. The beam hits the step walls and bounces off them (always parallel to the out-of plane axis). The springs are rigid to bending (can extend only in one direction) and are uncoupled. Thus, as the beam bounces off the step-walls elastically, it retains its vertical and horizontal energies (e_1, e_2) . Without the step, the system is a classical integrable system - all orbits belonging to a given level set (e_1, e_2) satisfy the Veech dichotomy: either all orbits are dense and cover the torus of angle variables uniformly (equi-distributed) or all orbits on this torus are closed. This behavior also implies that the return map to a transverse section of this torus is a rotation, and the rotation number on the prescribed level set determines which of the two options occurs. We show that this basic property is changed in the step-system. In particular, we identify a range of iso-energy level set surfaces that are of genus two and thus the return maps to a transverse section on such surfaces is, generally, a 5-IEM. This implies, for example, that an observable which depends on the oscillators phases (e.g. observable depending on the location of the beam) can have very delicate statistical properties [22, 14].

The paper is ordered as follows: in section 2 we define the step-system and state the main results: Theorem 2.1 which conjugates the step dynamics to the quasi-integrable dynamics of

directed motion on a genus-two torus and to L-shaped billiards, Corollary 2.2 which concludes that the energy surface has non-trivial foliation, Corollary 2.3 which concludes that including additional steps, staircases, strips and rectangular scatterers can be similarly analyzed, Theorem 2.4 which concludes that Poincaré return maps of the Hamiltonian impact step flow are conjugated, on each level set, to an IEM and Theorem 2.5 which summarises the results for the case of linear oscillators with impacts from a step. In section 3 we prove our main Theorem - that the motion in this system, on each level set, is conjugated to either a billiard flow, in a specific direction, on a rectangular domain, or to a billiard flow, in a specific direction, on an L-shaped billiard. Moreover, we prove that beyond a prescribed energy, the shape of the billiard on iso-energy surfaces changes from rectangular to continuously varying L-shaped billiards, back to rectangular domain, namely, that the topology of the invariant level set surfaces changes on iso-energy surfaces from genus one surfaces to genus two surfaces and back to genus one surfaces. In section 4 we define and compute (up to quadratures) the corresponding Poincaré return maps for the level-set dynamics (Theorems 4.1 and 4.2), namely, we provide an explicit proof of Theorem 2.4. Section 5 is devoted to establishing some specific properties of the resulting IEM, in particular, showing that typically there are many isolated level sets at which one of the intervals lengths vanishes. Section 6 applies these main results to linear oscillators, where the IEM are explicitly found, thus proving Theorem 2.5. We end with a discussion in which we list several natural extensions of this work and some open problems.

2 The step-system - setup and main results

Consider an autonomous C^r -smooth ($r \geq 3$) separable Hamiltonian corresponding to a particle motion in \mathbb{R}^2 :

$$H = H_1(q_1, p_1) + H_2(q_2, p_2) = \frac{p_1^2}{2m} + V_1(q_1) + \frac{p_2^2}{2m} + V_2(q_2) \quad (1)$$

where we assume for simplicity of presentation that the potentials $V_i(q)$ have a single simple minimum and are concave - they monotonically increase to infinity as $|q - q_{i,min}|$ increases (other interesting cases will be studied elsewhere). With no loss of generality, take the particle mass to be $m = 1$ and the potentials minima to be at $q_{i,min} = 0$ with $V_i(0) = 0$. For positive energies $e_i = H_i(q_i(t), p_i(t)) > 0, i = 1, 2$, the particle oscillates with frequencies $(\omega_1(e_1), \omega_2(e_2))$ in the box $[q_1^{min}(e_1), q_1^{max}(e_1)] \times [q_2^{min}(e_2), q_2^{max}(e_2)]$ of the configuration space, where $q_i^{min}(e_i)$ and $q_i^{max}(e_i)$ denote the minimal and maximal value of $q_i(t)$ on the level set e_i (so $V_i(q_i^{min}(e_i)) = V_i(q_i^{max}(e_i)) = e_i$). Since $q_{i,min} = 0$, for all positive e_i , $q_i^{min}(e_i) < 0 < q_i^{max}(e_i)$ and the level sets are nested $\frac{d}{de_i} q_i^{max}(e_i) > 0, \frac{d}{de_i} q_i^{min}(e_i) < 0$. Denote by $(\theta_i(t) = \omega_i(e_i)t + \theta_i(0), I_i(e_i))$ the action-angle coordinates of the 1 d.o.f. Hamiltonian $H_i(q_i, p_i) = H_i(I_i)$ (for one d.o.f. systems with concave potential these always exist and are unique up to a shift in the angle coordinate [1]).

A mechanical example of such a system is the beam held in a frame between two sets of uncoupled springs hinged on sliding, frictionless blocks (see Figure 1). The simplest case to consider is of Linear Oscillators (LO), namely, the case of quadratic potentials:

$$V_i^{LO}(q_i) = \frac{1}{2}\omega_i^2 q_i^2, \quad i = 1, 2. \quad (2)$$

We formulate below the main results (Theorems 2.1, Corollaries 2.2 and 2.3 and Theorem 2.4) for non-linear oscillators and dedicate Theorem 2.5 and section 6 to the LO case.

Now, introduce a step S in the configuration space (see Fig. 1):

$$S = \{(q_1, q_2) | q_1 < q_1^{wall} \text{ and } q_2 < q_2^{wall}\}, \quad q_1^{wall} \cdot q_2^{wall} \neq 0, \quad (3)$$

and assume the particle bounces off elastically from this step (we require, to avoid degeneracies, that the step is located away from the two axis); At the right wall of the step (hereafter, the 1-boundary), where $q_1 = q_1^{wall}$ and $q_2 < q_2^{wall}$, the horizontal momentum is switched $(q_1, q_2, p_1, p_2) \rightarrow (q_1, q_2, -p_1, p_2)$ whereas at the step upper wall (the 2-boundary), where $q_1 < q_1^{wall}$ and $q_2 = q_2^{wall}$, the vertical momentum changes sign $(q_1, q_2, p_1, p_2) \rightarrow (q_1, q_2, p_1, -p_2)$. When the particle hits the corner of the step the system is not defined and the trajectory stops. The flow is discontinuous at impacts, is smooth elsewhere, and the vertical and horizontal energies, e_i , are conserved by the impacts. We call this HIS the step system. Denote the step energies by

$$h_i^{step} = V_i(q_i^{wall}), \quad h^{step} = h_1^{step} + h_2^{step}, \quad (4)$$

the step-family of level sets by:

$$\mathcal{R}^c(h) = \{(e_1, e_2) | e_1 \in (h_1^{step}, h - h_2^{step}), \quad e_2 = h - e_1\}, \quad \text{defined for } h > h^{step}, \quad (5)$$

by $T_i(e_i) = \frac{2\pi}{\omega_i(e_i)}$ the period of the smooth oscillators, by

$$\Theta_2^{smooth} = \Theta_2^{smooth}(e_1, h) = 2\pi \frac{T_1(e_1)}{T_2(h - e_1)} \quad (6)$$

the rotation number of θ_2 on the level set $(e_1, e_2 = h - e_1)$, and by $\tilde{T}_i(e_i; q_i^{wall})$ the period of the impact system when it is reflected from a wall at $q_i = q_i^{wall}$ (namely, $\tilde{T}_i(e_i; q_i^{wall}) = 2 \int_{q_i^{wall}}^{q_i^{max}(e_i)} \frac{dq}{\sqrt{2(e_i - V_i(q_i))}}$). Finally, let

$$\theta_i^{wall}(e_i; q_i^{wall}) = \pi \frac{\tilde{T}_i(e_i; q_i^{wall})}{T_i(e_i)}. \quad (7)$$

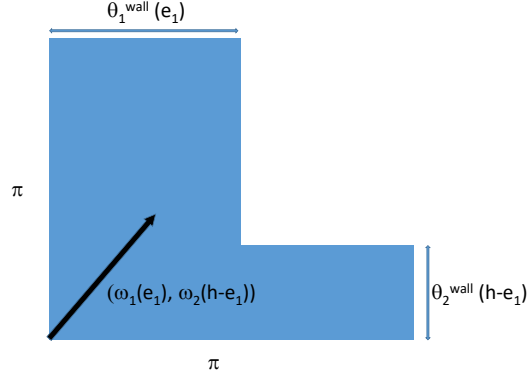


Figure 2: The directional flow on the L shaped billiard $L(\pi, \pi, \theta_1^{wall}(e_1; q_1^{wall}), \theta_2^{wall}(h - e_1; q_2^{wall}))$.

We will show later that by proper setting of the angle coordinate of the i th oscillator, $\theta_i^{wall}(e_i; q_i^{wall})$ is the angle variable phase at the wall (see Lemma 3.4). Depending on the properties of V_i and on the sign of q_i^{wall} , the functions $\theta_i^{wall}(e_i; q_i^{wall})$ may be monotone or not in e_i (for the LO case they are monotone, see below). Our main results are (see Fig 2):

Theorem 2.1. *Consider the step system: the two d.o.f. separable C^r ($r \geq 3$) smooth Hamiltonian of the mechanical form (1) where $(q_1, q_2) \in \mathbb{R}^2 \setminus S$ and trajectories reflect elastically at the step (3) boundaries. Assume each of the potentials $V_i(q_i)$ has a single minimum at the origin and is concave, namely, $qV'_i(q) > 0$ for all $q \neq 0$. Then, for all $h > h^{step}$, the flow on level sets belonging to the step family, $\mathcal{R}^c(h)$, is topologically conjugate to the $(\omega_1(e_1), \omega_2(h - e_1))$ - directional billiard flow on the L shaped billiard $L(\pi, \pi, \theta_1^{wall}(e_1; q_1^{wall}), \theta_2^{wall}(h - e_1; q_2^{wall}))$, and is thus not Liouville-integrable. In contrast, the step flow for the iso-energy level sets belonging to the complement of $\mathcal{R}^c(h)$ is topologically conjugate to a directional billiard flow on a rectangular billiard, namely it is Liouville integrable. For all $h > h^{step}$ both sets include intervals with non-empty interior.*

Corollary 2.2. *For all $h > h^{step}$ the foliation of the iso-energy surface to level sets with increasing e_1 value has two singularities at which the level sets topology changes: at $e_1 = h_1^{step}$ the topology changes from a genus one surface to a genus two surface whereas at $e_1 = h - h_2^{step}$ the topology changes back to a genus one surface.*

Corollary 2.3. *By adding more steps, staircases, strips and rectangular barriers to the reflecting set it is possible to create impact systems with level sets with any given genus ≥ 1 and any number of disconnected components. The corresponding iso-energy surfaces are foliated by a finite number of families of level sets with equi-genus and equi-number of components.*

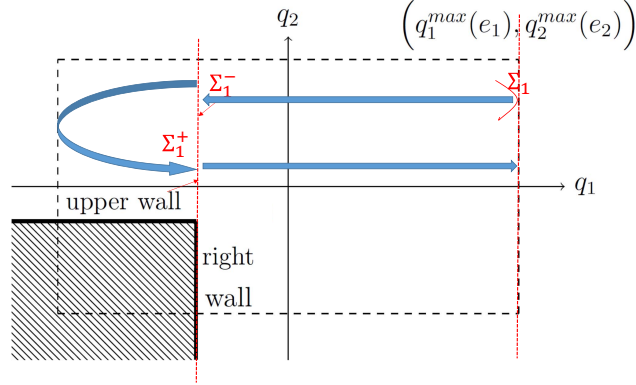


Figure 3: The return map geometry in configuration space.

Theorem 2.4. *Under the same conditions of Theorem 2.1, the return map to the section $\Sigma_1 = \{(q, p) | p_1 = 0, \dot{p}_1 < 0\}$ for each iso-energetic level set in $\mathcal{R}^c(h)$ is conjugated to an interval exchange map of three intervals on a circle. Restricting the angle to a natural fixed fundamental interval, for almost all level sets in $\mathcal{R}^c(h)$, the map becomes a five-interval exchange map (5-IEM). The return map to the section Σ_1 for iso-energy level sets in the complement of $\mathcal{R}^c(h)$ is a rotation on a circle, namely a 2-IEM.*

In section 4, explicit formulae (up to quadratures) for the return map at the iso-energy level sets $(e_1, h - e_1)$ are derived (for concreteness we consider the return map to Σ_1 - the analogous computations for the return map to Σ_2 amounts to replacing $1 \leftrightarrow 2$ in all definitions, and the same conclusions apply). These computations show that the numerical properties of three functions of e_1 (the functions $\theta_2^{wall}(h - e_1)$, $\Theta_2(e_1, h)$, $\chi_2(e_1, h)$ defined by Eq. (7,23,26)) determine the 5-IEM. In section 5 we discuss some properties of these functions and establish that there are isolated strongly resonant level sets at which orbits of different periods co-exist, level sets for which periodic and quasi-periodic motion co-exist, and, isolated level sets in $\mathcal{R}^c(h)$ at which the IEM reduces to a rotation (at these values the level set surface is a lattice surface). We believe all the other level sets have minimal dynamics and almost all of them have uniquely ergodic dynamics. Proving this conjecture, namely the genericity of the iso-energy curve of directional L-shaped billiard flows as in [11, 10], is beyond the scope of this paper.

For the linear oscillator step system, the period of the smooth motion does not depend on the energy, namely, $T_i(e_i) = \frac{2\pi}{\omega_i}$, and $q_i^{max}(e_i) = -q_i^{min}(e_i) = \sqrt{2e_i}/\omega_i$, hence all the functions which

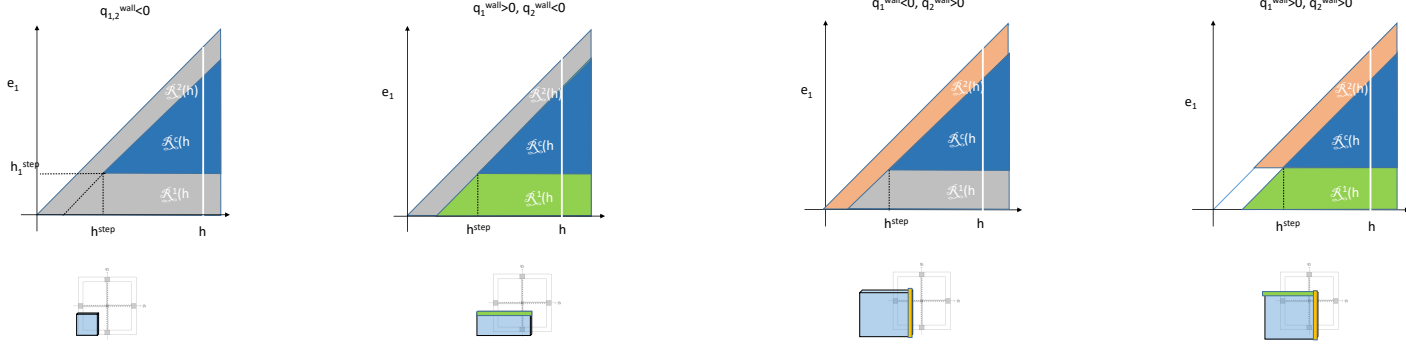


Figure 4: Impact-Energy momentum bifurcation diagram for the four relative positions of the step. The region where motion is allowed and no impacts occur (grey), the region where impacts occur at both sides of the step (blue) and the regions where impacts occur only at the upper (green) or right (orange) sides of the step are shown (see Lemmas 3.1-3.3).

determine the dynamics are explicit:

$$h^{step,LO} = \frac{1}{2}(\omega_1^2(q_1^{wall})^2 + \omega_2^2(q_2^{wall})^2) \quad (8)$$

$$\theta_i^{wall,LO}(e_i; q_i^{wall}) = \arccos \frac{\omega_i q_i^{wall}}{\sqrt{2e_i}} \in (0, \pi) \quad (9)$$

$$\Theta_2^{LO}(e_1) = 2 \frac{\omega_2}{\omega_1} \arccos \frac{\omega_1 q_1^{wall}}{\sqrt{2e_1}} \quad (10)$$

$$\chi_2^{LO}(e_1, h) = \frac{\omega_2}{\omega_1} \frac{(\pi - \arccos \frac{\omega_1 q_1^{wall}}{\sqrt{2e_1}})}{\arccos \frac{\omega_2 q_2^{wall}}{\sqrt{2(h-e_1)}}} \quad (11)$$

Theorem 2.5. *For $h > h^{step,LO}$, the flow of the Linear-Oscillators-step system on each level set in $\mathcal{R}^c(h)$ is topologically conjugated to the directional billiard flow in the fixed direction (ω_1, ω_2) on the L-shaped billiard $L(\pi, \pi, \theta_1^{wall,LO}(e_1; q_1^{wall}), \theta_2^{wall,LO}(h - e_1; q_2^{wall}))$. The L arms widths depend smoothly and monotonically on their arguments, and are of opposite monotonicity iff $q_1^{wall} q_2^{wall} > 0$. The return map to the section Σ_1 is an IEM of the form (31) with $(\theta_2^{wall}, \Theta_2, \chi_2) = (\theta_2^{wall,LO}(h - e_1; q_2^{wall}), \Theta_2^{LO}(e_1), \chi_2^{LO}(e_1, h))$ of Eqs (9,10,11).*

The proof and other properties of the step LO are presented in section 6.

3 The flow on level sets and the corresponding flat surfaces

In this section we prove Theorem 2.1. The main observation is that in terms of the smooth action angle coordinates, for the proper range of energies (the region $\mathcal{R}^c(h)$), impacts from the step correspond to a rectangular hole in the angle coordinates. Folding the torus according to the direction of motion in the configuration space leads to the motion in an L-shaped billiard with prescribed direction of motion and prescribed dimensions (up to quadratures). The rotational motion in the complimentary regions to $\mathcal{R}^c(h)$ follows from realizing that in these regions, for each level set, either there are no impacts at all or all impacts occur with only one side of the step.

Proof of Theorem 2.1: we first divide the level sets to three different classes according to the different types of impacts that may occur in each of them (lemmas 3.1-3.3). We then introduce the action-angle coordinates for the smooth system, fold them to the proper billiard table (an L-shaped table for level sets in $\mathcal{R}^c(h)$ and a rectangular table for the other level sets), and establish that the impacts from the step in the flow are mapped to impacts from the corresponding boundaries of the billiard table.

Delineating the energy level sets according to the impacts character:

In the next few lemmas we detail how the collisions with the step depend on both the energy in each direction and on the location of the step. This classification, which is summarized by Fig 4 and its implications are shown in Fig. 5, determines to which billiard table the flow on the level set is conjugated. Let

$$\mathcal{R}(h) = \{(e_1, e_2) | e_{1,2} > 0, e_1 + e_2 = h\}, \quad (12)$$

denote the open segment of allowed level set energy values on the isoenergy surface h (the white line in Fig 4) and by $\bar{\mathcal{R}}(h)$ the corresponding closed interval. For all $h > h^{step}$, the isoenergy step-collision set, $\mathcal{R}^c(h)$, is an open segment in the interior of $\mathcal{R}(h)$. Define the two iso-energy complementary closed segments:

$$\bar{\mathcal{R}}^i(h) = \{(e_1, e_2) | 0 \leq e_i \leq \min\{h, h_i^{step}\}, e_{\bar{i}} = h - e_i\}, \quad (13)$$

(with interior open segments, $\mathcal{R}^i(h)$) where, hereafter, we denote by \bar{i} the complement d.o.f. to i (namely $\bar{1} = 2, \bar{2} = 1$). Fig. 4 shows these sets in the energy-momentum diagram for different locations of the walls.

Lemma 3.1. *All trajectories belonging to level sets in $\mathcal{R}^i(h)$ do not hit the i -boundary. For $0 < h < h^{step}$, $\mathcal{R}(h) = \mathcal{R}^1(h) \cup \mathcal{R}^2(h)$ and the segment $\bar{\mathcal{R}}^1(h) \cap \bar{\mathcal{R}}^2(h)$ is non-empty. For all $h > h^{step}$, $\bar{\mathcal{R}}(h) = \bar{\mathcal{R}}^1(h) \cup \mathcal{R}^c(h) \cup \bar{\mathcal{R}}^2(h)$ and these three segments are non-empty and disjoint.*

Proof. Since the potentials are concave the level sets are nested. Level sets in the interior of $\mathcal{R}^i(h)$ satisfy $e_i < h_i^{step}$, hence, for all t , the trajectories satisfy: $q_i(t; e_i) \in [q_i^{min}(e_i), q_i^{max}(e_i)] \subset$

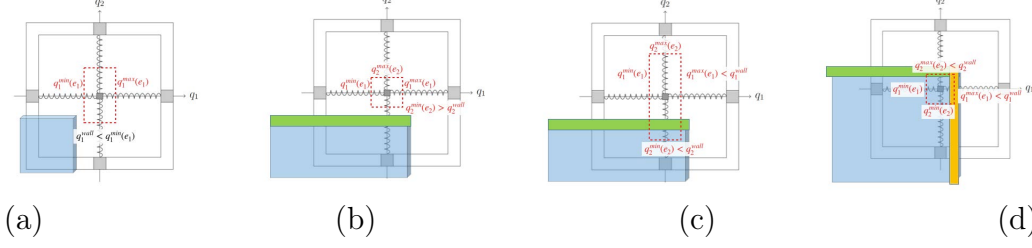


Figure 5: The level sets projection to the configuration space (dashed red box) for level sets in \mathcal{R}^1 (see Lemmas 3.1 and 3.2); (a) No impacts: $q_{1,2}^{wall} < 0, (e_1, e_2) \in \mathcal{R}^1$, (b) No impacts: $q_1^{wall} > 0, q_2^{wall} < 0, (e_1, e_2) \in \mathcal{R}^1 \cap \mathcal{R}^2$, (c) Impacts only with the 2-boundary (upper boundary) $q_1^{wall} > 0, q_2^{wall} < 0, (e_1, e_2) \in \mathcal{R}^1 \setminus \mathcal{R}^2$, (d) No motion for this level set: $q_1^{wall} > 0, q_2^{wall} > 0, (e_1, e_2) \in \mathcal{R}^1 \cap \mathcal{R}^2$.

$(q_i^{min}(h_i^{step}), q_i^{max}(h_i^{step}))$. By definition, $q_i^{wall} \in \{q_i^{min}(h_i^{step}), q_i^{max}(h_i^{step})\}$ so such trajectories do not cross the line $q_i = q_i^{wall}$ and the step i th boundary cannot be impacted. The rest of the lemma follows from the definitions of $\mathcal{R}(h), \mathcal{R}^{1,2}(h), \mathcal{R}^c(h)$ (Eqs. 12,13,5), see also Fig. 4. \square

Fig. 5 demonstrates that in accordance with lemma 3.1, level sets that belong to $\mathcal{R}^1(h)$ do not impact the 1-boundary (the right side of the step). Next we establish when such level sets impact the 2-boundary (the upper side of the step):

Lemma 3.2. *If $q_i^{wall} < 0$, trajectories associated with level sets in $\mathcal{R}^i(h)$ do not hit the step. If $q_i^{wall} > 0$, the dynamics in $\mathcal{R}^i(h)$ is further divided to the following two cases:*

For level sets in $\mathcal{R}^i(h) \setminus \bar{\mathcal{R}}^i(h)$: *trajectories hit the \bar{i} -boundary only, and the impacts are transverse.*

For level sets in $\mathcal{R}^1(h) \cap \mathcal{R}^2(h)$: *trajectories do not hit the step if $q_i^{wall} < 0$ and are not in the allowed region of motion if $q_i^{wall} > 0$.*

Proof. If (e_1, e_2) belong to $\mathcal{R}^i(h)$ then $e_i < h_i^{step}$ (see (13)). If additionally, $q_i^{wall} < 0$, then $q_i^{min}(e_i) > q_i^{wall}$, so the oscillation in the i th direction do not reach the wall, independently of the oscillation amplitude in the \bar{i} direction (see Fig 5(a)).

If $q_i^{wall} > 0$, then $q_i^{max}(e_i) < q_i^{wall}$, so, while impacts cannot occur with the i boundary, transverse impacts with the \bar{i} boundary occur when $e_{\bar{i}} > h_{\bar{i}}^{step}$, namely when $(e_1, e_2) \in \mathcal{R}^i(h) \setminus \bar{\mathcal{R}}^i(h)$ (see Fig 5(b)).

If $q_i^{wall} > 0$ and $e_{\bar{i}} < h_{\bar{i}}^{step}$, so $(e_1, e_2) \in \mathcal{R}^1(h) \cap \mathcal{R}^2(h)$, the \bar{i} boundary cannot be crossed. If, additionally, $q_i^{wall} < 0$, then $e_{\bar{i}} < h_{\bar{i}}^{step}$ implies that $q_i^{min}(e_{\bar{i}}) > q_i^{wall}$ and the oscillations are in the allowed region of motion and do not hit the step (see Fig 5(c)), whereas if $q_i^{wall} > 0$ then $q_i^{max}(e_{\bar{i}}) < q_i^{wall}$ and the motion is "behind the step" namely it is not in the allowed region of motion (see Fig 5(d)). \square

Lemma 3.3. *Each level set in the step collision set, $\mathcal{R}^c(h)$, includes trajectories which impact transversely the 1-boundary and trajectories which impact transversely the 2-boundary.*

Proof. Consider $(e_1, e_2) \in \mathcal{R}^c(h)$. Then, the corresponding level sets in each d.o.f. include the step position, namely, $q_i^{min}(e_i) < q_i^{wall} < q_i^{max}(e_i)$, $i = 1, 2$. Denote hereafter the smooth Hamiltonian flow by $\varphi_t^{smooth}(z)$ where $z = (q_1, q_2, p_1, p_2)$. The open, one dimensional set of i.c. $Z_1 = \{z | z = (q_1^{wall}, q_2, -\sqrt{2(e_1 - h_1^{step})}, \pm\sqrt{2(e_2 - V_2(q_2))}), q_2 \in (q_2^{min}(e_2), q_2^{wall})\}$ is non-empty and belongs, by construction, to the level set (e_1, e_2) . Its projection to the configuration space belongs to the right, 1-boundary of the step. Hence, for sufficiently small t , the set $\varphi_{-t}(Z_1)$ is within the allowed region of motion, belongs to the level set $(e_1, e_2) \in \mathcal{R}^c(h)$, and consists of i.c. which impact at time t the 1-boundary of the step transversely, with horizontal velocity $-\sqrt{2(e_1 - h_1^{step})}$. Similarly, defining $Z_2 = \{z | z = (q_1, q_2^{wall}, \pm\sqrt{2(e_1 - V_1(q_1))}, -\sqrt{2(e_2 - h_2^{step})}), q_1 \in (q_1^{min}(e_1), q_1^{wall})\}$, the set $\varphi_{-t}(Z_2)$ is within the allowed region of motion for sufficiently small t and consists of i.c. belonging to the level set $(e_1, e_2) \in \mathcal{R}^c(h)$ which impact at time t the 2-boundary of the step transversely, with vertical velocity $-\sqrt{2(e_2 - h_2^{step})}$. \square

While, for most cases ("non-resonant"), each trajectory belonging to level sets $(e_1, e_2) \in \mathcal{R}^c(h)$ hits both boundaries of the step many times, in some resonant cases, it is possible to have families of trajectories belonging to level sets $(e_1, e_2) \in \mathcal{R}^c(h)$ that hit only one of the step boundaries or even avoid collisions (resonant trajectories belonging to the interval J_K of (31) with $K = 0$, see section 4 for more details).

Action angle coordinates and transverse sections:

The action angle coordinates of the 1 d.o.f. Hamiltonian, $H_i(q_i, p_i)$, $(I_i, \theta_i(t) = \omega_i(I_i)t + \theta_i(0))$, are uniquely defined up to a shift in the angle. Since By our assumptions $H_i(I_i) = e_i$ is invertible, e_i or I_i may be used to label level sets (to simplify notation, we hereafter consider the frequencies as functions of the energies, e_i). By the monotonicity of $V_i(q_i)|_{q_i \neq 0}$, for all energy surfaces $h = e_1 + e_2 > 0$, each energy surface contains a family of invariant tori on which rotations occur, and its boundary consists of the two invariant circles that correspond to the normal modes - the oscillatory motion of only one oscillator with the other one at rest ($e_1 = 0, e_2 = h$ and $e_1 = h, e_2 = 0$).

For $e_i > 0$, denote by Σ_i the three dimensional transverse section $\{p_i = 0, \dot{p}_i < 0\}$, and we set the phases of the action-angle coordinates to vanish on the section (so $\theta_i = 0 \pmod{2\pi}$ on Σ_i):

$$\Sigma_i : \{(q_i, \bar{q}_i, p_i, \bar{p}_i) | p_i = 0, \dot{p}_i < 0\} = \{(\theta_i, \bar{\theta}_i, I_i, \bar{I}_i) | \theta_i = 0, I_i > 0\}. \quad (14)$$

By the symmetry of the mechanical Hamiltonian, with this choice of the phases, $p_i(t) > 0$ for $\theta_i(t) \in (-\pi, 0) \pmod{2\pi}$ and similarly $p_i(t) < 0$ for $\theta_i(t) \in (0, \pi) \pmod{2\pi}$, namely $sign(p_i(t)) = sign(\dot{q}_i(t)) = -sign(\theta_i(t) \pmod{2\pi})$. For p_i which is bounded away from zero, the smooth flow is smoothly conjugate, through the action angle transformation, to the directional motion on the flat torus in the direction $(\omega_1(e_1), \omega_2(e_2))$. The directed motion on the torus is conjugated, by standard

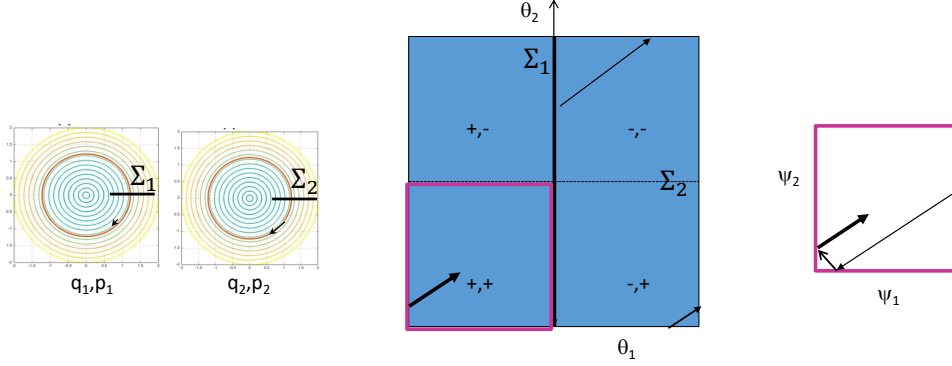


Figure 6: Folding the smooth flow to a billiard: the motion on a level set is conjugated via action angle coordinated to the directional motion on the angles-torus. The motion is conjugated to the directional billiard motion on the left lower square. The direction of motion in this billiard is in the same quadrant as the direction of motion in the configuration space (see Eq. (15)).

folding, to the directed billiard motion on the square $(\psi_1, \psi_2) \in [-\pi, 0] \times [-\pi, 0]$ (see figure 6). For this specific folding and for the choice of the angle phase (14), the direction of time is preserved along trajectories of the smooth flow and the billiard:

$$\text{sign}(p_i(t)) = \text{sign}(\dot{q}_i(t)) = \text{sign}(\dot{\psi}_i(t)) \quad (15)$$

namely, the directed billiard in the square (hereafter called the ψ -billiard) and the smooth flow on the level set (e_1, e_2) are topologically conjugated, see Fig 6. By reflections and time reversal, the flow is also conjugated to the billiard on the positive quadrant.

We use the same construction of conjugacy for the impact system. Let:

$$\Sigma_i^\pm = \{(q, p) | q_i = q_i^{wall}, \pm p_i > 0\}, \quad (16)$$

and let $t_{\Sigma_i^- \rightarrow \Sigma_i^+} = T_i(e_i^{wall}) - \tilde{T}_i(e_i; q_i^{wall})$, $t_{\Sigma_i^+ \rightarrow \Sigma_i^-} = t_{\Sigma_i \rightarrow \Sigma_i^-} = \frac{1}{2}\tilde{T}_i(e_i; q_i^{wall})$ denote the respective travel times between the sections.

Lemma 3.4. *The sections Σ_i^\pm are impacted/crossed transversely by the step-flow if and only if $e_i > h_i^{step}$. For all i.c. belonging to a level set $e_i > h_i^{step}$, with the angle coordinate convention (14),*

the angle θ_i at the section Σ_i^- is $\theta_i^{wall}(e_i)$:

$$\theta_i^{wall}(e_i; q_i^{wall}) = \omega_i(e_i) t_{\Sigma_i \rightarrow \Sigma_i^-} = \omega_i(e_i) \int_{q_i^{wall}}^{q_i^{max}(e_i)} \frac{dq}{\sqrt{2(e_i - V_i(q_i))}} = \pi \frac{\tilde{T}_i(e_i; q_i^{wall})}{T_i(e_i; q_i^{wall})}, \quad (17)$$

and a reflection from the step at q_i^{wall} sends the angle $\theta_i^{wall}(e_i; q_i^{wall})$ to $2\pi - \theta_i^{wall}(e_i; q_i^{wall}) = -\theta_i^{wall}(e_i; q_i^{wall}) \bmod 2\pi$.

Proof. Since the level sets of H_i are nested, for $e_i < h_i^{step}$ the e_i level set is strictly interior to the h_i^{step} level set, and hence the sections Σ_i^\pm are not reached by the flow. Conversely, for $e_i > h_i^{step}$, the sections Σ_i^\pm are crossed by the level set, and, by the mechanical form of the Hamiltonian H_i , on these sections $p_i^2 = 2(e_i - V(q_i^{wall})) > 0$ so they are crossed transversely. The formula for $\theta_i^{wall}(e_i; q_i^{wall})$ follows from the definition of action-angle coordinates and the convention (14). By the symmetry $p_i \rightarrow -p_i$ of mechanical Hamiltonian function it follows that the reflection from the step at q_i^{wall} sends the wall angle coordinate θ_i^{wall} to $2\pi - \theta_i^{wall}(e_i) = -\theta_i^{wall}(e_i) \bmod 2\pi$. \square

Notice that, as summarized in Table 1,

$$\lim_{e_i \searrow h_i^{step}} \theta_i^{wall}(e_i; q_i^{wall}) = \begin{cases} \pi & \text{for } q_i^{wall} < 0 \\ 0 & \text{for } q_i^{wall} > 0. \end{cases} \quad (18)$$

and

$$\lim_{e_i \rightarrow \infty} \theta_i^{wall}(e_i; q_i^{wall}) = \theta_i^{wall, \infty}, \quad (19)$$

where, for symmetric potentials, $\theta_i^{wall, \infty} = \frac{\pi}{2}$.

Combining the classification of level sets according to their impacts with the boundaries (lemmas 3.1-3.3) with the action-angle representation of the flow and the impacts on a given level set (lemma 3.4), we establish the topological conjugacy between the impact flow on a given level set and its corresponding flat surface and billiard table. To this aim, it is convenient to define:

$$\hat{\theta}_i^{wall}(e_i, e_{\bar{i}}; q_i^{wall}, q_{\bar{i}}^{wall}) = \begin{cases} \emptyset & \text{if } q_{1,2}^{wall} > 0 \wedge e_{1,2} < h_{1,2}^{step} \\ \theta_i^{wall}(e_i; q_i^{wall}) & \text{if } e_i \geq h_i^{step} \wedge (e_{\bar{i}} \geq h_{\bar{i}}^{step} \vee q_{\bar{i}}^{wall} > 0) \\ \pi & \text{otherwise.} \end{cases} \quad (20)$$

By lemmas 3.1-3.3, $\hat{\theta}_i^{wall}(e_i, e_{\bar{i}}; q_i^{wall}, q_{\bar{i}}^{wall}) = \theta_i^{wall}(e_i; q_i^{wall})$ for level sets for which impacts (transverse or tangent) with the i -boundary are allowed, $\hat{\theta}_i^{wall}(e_i, e_{\bar{i}}; q_i^{wall}, q_{\bar{i}}^{wall}) = \emptyset$ for level sets that are not in the allowed region of motion, and $\hat{\theta}_i^{wall}(e_i, e_{\bar{i}}; q_i^{wall}, q_{\bar{i}}^{wall}) = \pi$ for level sets in which impacts with the i -th boundary cannot occur.

Rotational dynamics for level sets in $\bar{\mathcal{R}}^i(h)$:

Lemma 3.5. *For level sets (e_1, e_2) in $\bar{\mathcal{R}}^i(h)$ the step-dynamics are smoothly conjugate to the directional motion $(\omega_i(e_i), \omega_{\bar{i}}(e_{\bar{i}}))$ on the two-torus*

$$\mathbb{T}_i(e_1, e_2) = \{(\theta_i, \theta_{\bar{i}}) | \theta_i \in [-\pi, \pi), \theta_{\bar{i}} \in [-\hat{\theta}_i^{wall}, \hat{\theta}_i^{wall})\}, \quad (21)$$

with $\hat{\theta}_{\bar{i}}$ defined by (20). This step-dynamics are also conjugated to the $(\pm\omega_i(e_i), \pm\omega_{\bar{i}}(e_{\bar{i}}))$ directional billiard motion on the rectangular billiard $(\psi_i, \psi_{\bar{i}}) \in [-\pi, 0] \times [-\hat{\theta}_{\bar{i}}^{wall}, 0]$. In particular, the conjugation keeps the direction of motion: the signs of $\psi_{1,2}$ and the sign of $\dot{q}_{1,2}$ coincide.

Proof. By lemma 3.2 the motion on level sets in $\mathcal{R}^i(h)$ is either: a) not defined (so $\hat{\theta}_i^{wall} = \emptyset$), b) corresponds to reflections only from the \bar{i} - boundary of the step, or, c) the trajectory does not touch the step, so the motion occurs as in the non-impact case on the torus (21) with $\hat{\theta}_i^{wall} = \pi$.

The three rows of conditions in the definition (20) of $\hat{\theta}_i^{wall}$ for $e_i < h_i^{step}$ coincide with the conditions listed for cases a,b,c in lemma 3.2, so, to complete the proof we only need to show that case b) indeed corresponds to the rotation on the clipped torus (21) with $\hat{\theta}_i^{wall} = \theta_i^{wall}$. Indeed, by the mechanical form of $H_{\bar{i}}$, reflections only from the \bar{i} - boundary of the step imply that the corresponding angle coordinate is restricted to the interval $\theta_{\bar{i}}(t) \in [-\theta_{\bar{i}}^{wall}(e_{\bar{i}}; q_{\bar{i}}^{wall}), \theta_{\bar{i}}^{wall}(e_{\bar{i}}; q_{\bar{i}}^{wall})]$, where, by lemma 3.4, the transverse impacts correspond to gluing the transverse section $\Sigma_{\bar{i}}^{\pm}|_{H_{\bar{i}}=e_{\bar{i}}}$:

$$\Sigma_{\bar{i}}^-|_{H_{\bar{i}}=e_{\bar{i}}} = \{(\theta, I) | I_{\bar{i}} = I_{\bar{i}}(e_{\bar{i}}), \theta_{\bar{i}} = \theta_{\bar{i}}^{wall}(e_{\bar{i}})\}, \quad \Sigma_{\bar{i}}^+|_{H_{\bar{i}}=e_{\bar{i}}} = \{(\theta, I) | I_{\bar{i}} = I_{\bar{i}}(e_{\bar{i}}), \theta_{\bar{i}} = -\theta_{\bar{i}}^{wall}(e_{\bar{i}})\}. \quad (22)$$

by identifying the angles $\theta_{\bar{i}}^{wall}(e_{\bar{i}}; q_{\bar{i}}^{wall})$ and $-\theta_{\bar{i}}^{wall}(e_{\bar{i}}; q_{\bar{i}}^{wall})$. Namely, we obtain a directional motion on the torus (21), in the direction $(\omega_i(e_i), \omega_{\bar{i}}(e_{\bar{i}}))$. By folding to the rectangle $(\psi_i, \psi_{\bar{i}}) \in [-\pi, 0] \times [-\hat{\theta}_{\bar{i}}^{wall}, 0]$, the motion is conjugated to the ψ -billiard in this rectangular billiard, and (15) holds for the impact flow as well, proving the lemma for this case as well, see tables IIA,IIIA,IIID,IIID of Fig. 7. \square

The flow in the region $\mathcal{R}^c(h)$ is conjugated to the L-shaped billiard flow:

Lemma 3.6. *For level sets (e_1, e_2) in $\mathcal{R}^c(h)$ the step-dynamics are conjugate to the directional motion $(\omega_1(e_1), \omega_2(e_2))$ on SW - the swiss-cross-shaped (θ_1, θ_2) -surface with vertical arms of width $2\theta_1^{wall}(e_1)$ and length 2π , horizontal arms of height $2\theta_2^{wall}(e_2)$ and width 2π and the flat surface is achieved by gluing of parallel opposite sides. This step-dynamics are also conjugate to the $(\pm\omega_i(e_i), \pm\omega_{\bar{i}}(e_{\bar{i}}))$ directional billiard motion on the L-shaped billiard $L(\pi, \pi, \theta_1^{wall}(e_1; q_1^{wall}), \theta_2^{wall}(h - e_1; q_2^{wall}))$. Reflecting the L-shaped billiard with respect to the θ_1 -axis and the θ_2 -axis provides dynamics with conjugation that keeps the direction of motion.*

Proof. Recall that with the convention (14), $q_i(t; e_i) > q_i^{wall}$ iff the angle coordinate of the smooth flow is in the interval $(-\theta_i^{wall}(e_i; q_i^{wall}), \theta_i^{wall}(e_i; q_i^{wall}))$. Hence, on a level set $(e_1, e_2) \in \mathcal{R}^c(h)$,

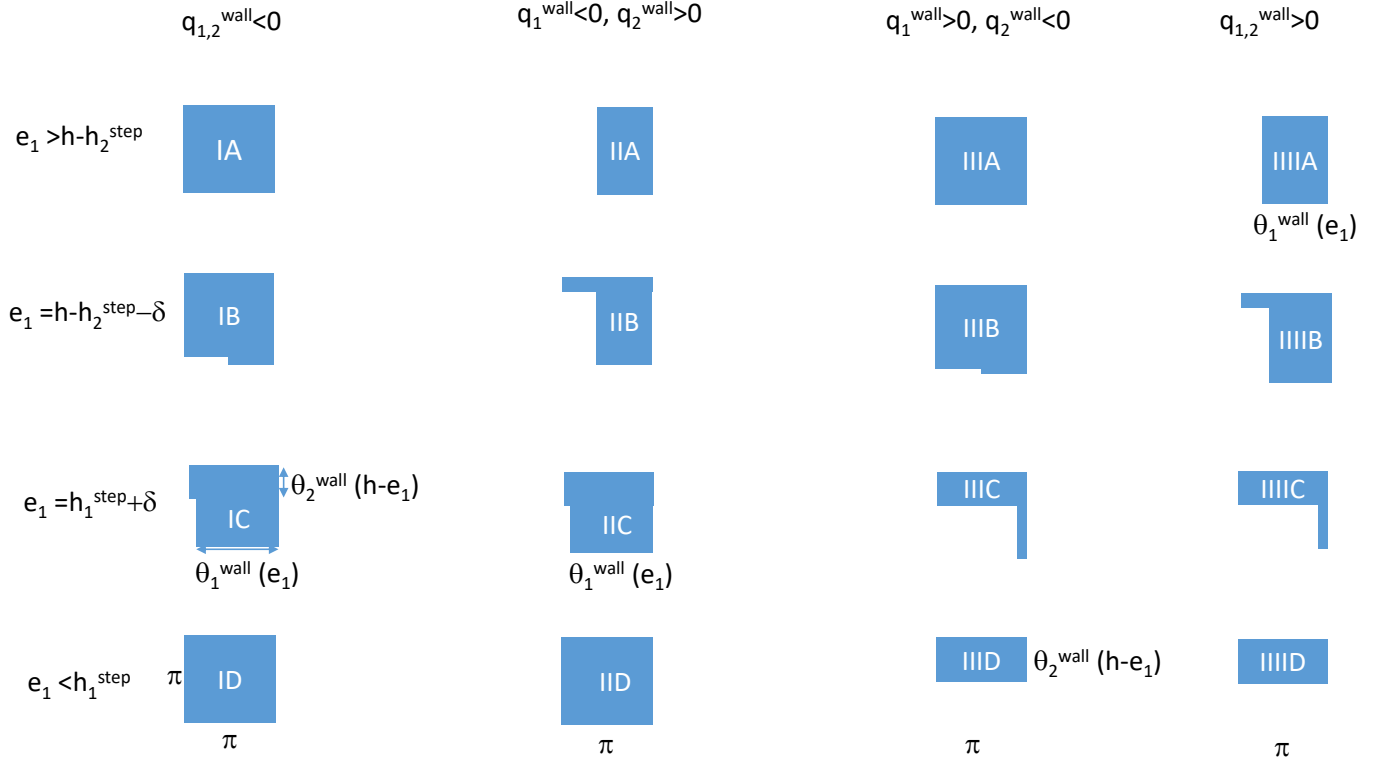


Figure 7: The iso-energy billiard geometry at the different step locations for $h > h^{\text{step}}$. The first and last rows present, respectively, the rectangular billiards for level sets in $\mathcal{R}^2(h)$ and $\mathcal{R}^1(h)$. The second and third rows present, respectively, the L-shaped billiards in $\mathcal{R}^c(h)$ just below and just above the edges of the $\mathcal{R}^c(h)$ interval (so $\delta > 0$ is small).

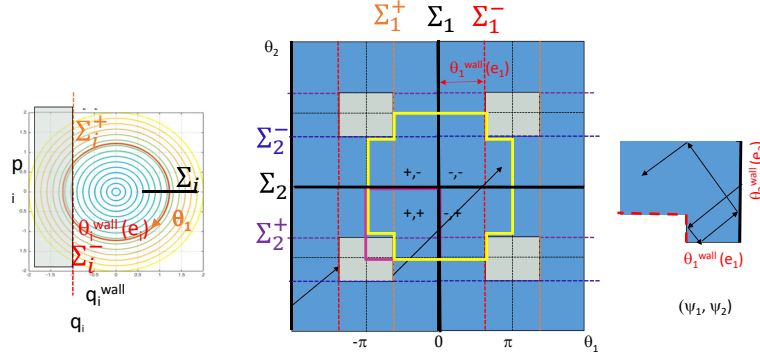


Figure 8: The step return map, the swiss cross surface and the rotated L-shaped billiard geometry for level sets in the step region, $\mathcal{R}^c(h)$. The grey areas correspond to the step region in the angles space. The yellow outlines the boundary of SW, the Swiss-cross flat surface for which opposite parallel sides are glued.

the disallowed step region in the configuration space is mapped by the smooth action-angle transformation to a disallowed rectangular region in the angle variables: $(\theta_1, \theta_2) \in S_{\theta(e_1, e_2)} := [\theta_1^{wall}(e_1; q_1^{wall}), 2\pi - \theta_1^{wall}(e_1; q_1^{wall})] \times [\theta_2^{wall}(e_2; q_2^{wall}), 2\pi - \theta_2^{wall}(e_2; q_2^{wall})]$ all taken mod 2π . This rectangle cuts the four corners of the fundamental domain creating a swiss cross surface (see Fig. 8). By lemma 3.4, the reflection rule at impact, $p_i \rightarrow -p_i$, translates to $\theta_i^{wall} \rightarrow 2\pi - \theta_i^{wall}$. Hence, the resulting flow under the step dynamics, expressed in the smooth action angle coordinates, corresponds to setting the action values to constants, $I_i(e_i)$, and letting the angles (θ_1, θ_2) increase linearly at constant speeds $(\omega_1(e_1), \omega_2(e_2))$ on the two torus $[0, 2\pi] \times [0, 2\pi]$, till the rectangle $S_{\theta(e_1, e_2)}$ is met. There, the gluing condition $\theta_i^{wall}(e_i; q_i^{wall}) \rightarrow 2\pi - \theta_i^{wall}$ is applied, namely, this is a flow on a flat torus with a rectangular hole, or, equivalently, when shifting the torus center by $(-\pi, -\pi)$, on a swiss-cross surface, see Figure 8. For all $(e_1, e_2 = h - e_1) \in \mathcal{R}^c(h)$, the dynamics under this gluing rule of the swiss-cross correspond to an unfolding of a billiard motion in the $\mathbf{B}(e_1) = L(\pi, \pi, \theta_1^{wall}(e_1; q_1^{wall}), \theta_2^{wall}(h - e_1; q_2^{wall}))$ -shaped table [2, 27] in the directions $(\pm\omega_1(e_1), \pm\omega_2(h - e_1))$, where, as before, by the choice (14) of the angle phases, (15) holds on the L-shaped billiard that is folded onto the low-left part of the swiss cross (see Fig 8 and Fig. 9). Thus, we have shown that the dynamics on the iso-energetic level sets in $\mathcal{R}^c(h)$ are conjugated to the family of α -directional flows on the family of L-shaped billiards, $\mathcal{B}(h) = \{\alpha(e_1) = \frac{\omega_2(h - e_1)}{\omega_1(e_1)}, \mathbf{B}(e_1)\}_{|e_1 \in \mathcal{I}^c(h)}$, where $\mathcal{I}^c(h) := (h_1^{step}, h - h_2^{step} = h_1^{step} + h - h^{step})$. \square

Since the motion on a genus-2 surface is not Liouville integrable, Lemmas 3.5 and 3.6 complete

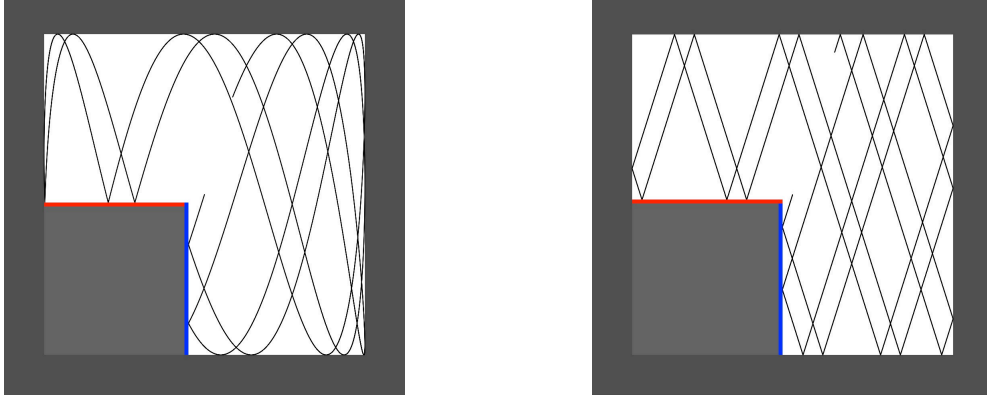


Figure 9: A simulation of the configuration space of the linear oscillators step system (left) with its corresponding matching L-shaped billiard in the angle space (right). The turning points of the flow, where $p_i = 0$, are mapped to reflections from the outer square boundaries and the elastic reflections of the flow from the step are mapped to the billiard reflections from the step.

the proof of Theorem 2.1.

Each column of Fig. 7 shows schematically the family of iso-energetic billiard tables obtained for the indicated positions of the step. The directional L-shaped billiard families, $\mathcal{B}(h)$, are shown in rows B and C and correspond to level sets in $\mathcal{R}^c(h)$. The widths of the arms of L-shaped tables at the edges of the segment $\mathcal{R}^c(h)$ (these depend on the signs of $q_{1,2}^{wall}$) are listed in Table 1 - note that they are distinct, namely, for all $h > h^{step}$, $\theta_i^{wall}(h_i^{step}) \neq \theta_i^{wall}(h - h_i^{step})$. The rectangular billiards shown in rows A and D correspond to level sets in $\mathcal{R}^1(h)$ and $\mathcal{R}^2(h)$ respectively.

Lemma 3.4 in the above proof exposes the simple relation between reflections from vertical and horizontal boundary segments and the corresponding gluing rule in the angles variables. Corollaries 2.2 and 2.3 follow from this construction; steps (two rays meeting at a $\frac{3\pi}{2}$ corner) produce for sufficiently high individual energies a single hole, a staircase in the configuration space creates at sufficiently high individual energies a nibbled hole in the angles variables, a strip with handles creates, for intermediate individual energies several disconnected components and for sufficiently high individual energies two holes, and a rectangle creates for sufficiently high individual energies four holes, see Fig. 10 for a demonstration. Thus, by constructing a nibbled scattering geometry which combines finite and semi-infinite horizontal and vertical segments in the configuration space, the number of holes and the number of connected components in the iso-energy level set surfaces can be manipulated. Moreover, constructing an impact energy-momentum diagram [19, 20], such as Fig 4 for the one-step system, allows to identify the critical energy values at which the topology of the energy surface changes.

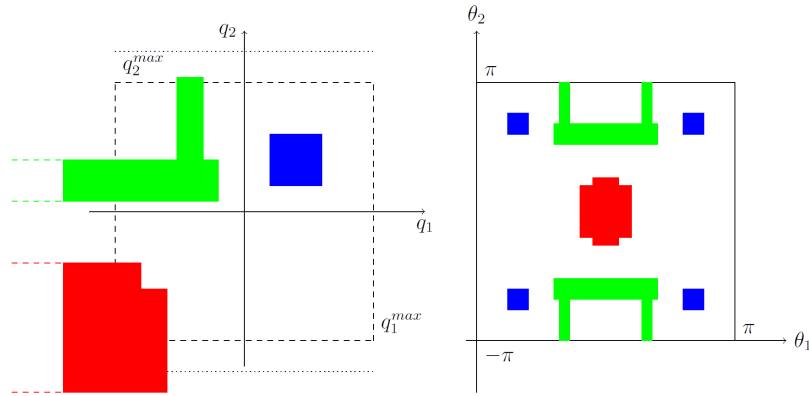


Figure 10: For the indicated level set (dashed line), a 2-step staircase (red), a strip with a handle (green) and a block (blue) in the configuration space (left figure) create, respectively, one, one and four holes in the angle-angle torus representation, and divide the torus to two disconnected components (inside and outside of the green frame). A slight increase in the vertical energy e_2 (dotted lines) makes the level set surface connected with two green holes.

Corner position	$\theta_1^{wall}(h_1^{step})$	$\theta_2^{wall}(h - h_1^{step})$	$\theta_1^{wall}(h - h_2^{step})$	$\theta_2^{wall}(h_2^{step})$
$q_{1,2}^{wall} < 0$	π	$\theta_2^{wall}(h - h_1^{step}; q_2^{wall})$	$\theta_1^{wall}(h - h_2^{step}; q_1^{wall})$	π
$q_1^{wall} < 0, q_2^{wall} > 0$	π	"	"	0
$q_1^{wall} > 0, q_2^{wall} < 0$	0	"	"	π
$q_{1,2}^{wall} > 0$	0	"	"	0

Table 1: The values of $\theta_{1,2}^{wall}$ at the two edges of $\mathcal{R}^c(h)$, see rows B,C of Fig. 7.

4 Return maps

Proof of Theorem 2.4 In Theorem 2.1 we proved that the step dynamics on each iso-energy level set is conjugated, via the action angle transformation, to the $(\omega_1(e_1), \omega_2(h - e_1))$ directional flow on a flat surface - a glued swiss cross for level sets in $\mathcal{R}^c(h)$ (lemma 3.6) and a torus for level sets in the complement to $\mathcal{R}^c(h)$ (lemma 3.5). The transverse Poincaré section Σ_1 of the step flow is conjugated to the transverse section $\theta_1 = 0$ on these surfaces via the action-angle transformation (recall (14), and notice that the assumptions on the potentials imply that $\omega_1(e_1)$ is bounded away from zero for any finite e_1), so the return map of the step flow to Σ_1 is conjugated to the return map to Σ_1 on the corresponding flat surface. The return map to Σ_1 on the flat surface is an interval exchange map on a circle: for the swiss cross a three-interval exchange map and for the torus a rotation of a single interval (see, e.g. [27]). For a fixed fundamental interval on this circle, the return map becomes, in general, a 5-IEM for the swiss-cross case and a 2-IEM for the torus. Computations of the resulting IEMs (see Theorems 4.2) show that the lengths of the intervals of the 5-IEMs and their positions on the circle for iso-energy level sets change smoothly in the step region. In particular, conditions for having a zero length interval are expressed as an equation of smooth, non-constant functions of e_1 which can vanish only at isolated e_1 values in the interior of $\mathcal{R}^c(h)$.

Next, we calculate the iso-energetic family of IEMs, $\mathcal{F}(h) = \{F = F_{(e_1, h - e_1)}\}_{e_1 \in [0, h]}$ for the 2-IEM case (Theorem 4.1) and for the 5-IEM case (Theorem 4.2) thus completing the proof of Theorem 2.4. In section 5 we explore some of the properties of the 5-IEM family.

Let Θ_2 denote the gain in the θ_2 phase of the return map to Σ_1 when the motion is to the right of the step:

$$\Theta_2 = \Theta_2(e_1, h; q_{1,2}^{wall}) = \frac{\hat{\theta}_1^{wall}}{\pi} \Theta_2^{smooth} = \begin{cases} 2\pi \frac{\tilde{T}_1(e_1; q_1^{wall})}{T_2(h - e_1)} & \text{if } \hat{\theta}_1^{wall}(e_1, h; q_{1,2}^{wall}) \neq \pi \\ \Theta_2^{smooth}(e_1, h) & \text{if } \hat{\theta}_1^{wall}(e_1, h; q_{1,2}^{wall}) = \pi, \end{cases} \quad (23)$$

where $\hat{\theta}_1^{wall}(e_1, h; q_{1,2}^{wall})$ (see Eq. (20)) is the effective impact angle with the side boundary of the step and $\Theta_2^{smooth}(e_1, h)$ (see Eq. (6)) is the rotation in θ_2 for non-impacting trajectories. Notice

that for all level sets on which motion is defined $\Theta_2 \leq \Theta_2^{smooth}$. Let

$$\Theta_2^*(e_1, h; q_{1,2}^{wall}) = 2\hat{\theta}_2^{wall} \left\{ \frac{\Theta_2}{2\hat{\theta}_2^{wall}} \right\} \quad (24)$$

where $\{x\}$ denotes hereafter the fractional part of the number x . We first establish that in the complementary sets to $\mathcal{R}^c(h)$ the return map to Σ_1 is the rotation (25):

Theorem 4.1. *Under the same conditions of Theorem 2.1, for all iso-energy level sets in $\mathcal{R}^1(h) \cup \mathcal{R}^2(h)$, the return map $F_{(e_1, h-e_1)}$ to the section Σ_1 is topologically conjugated to a Θ_2 rotation on the $[-\hat{\theta}_2^{wall}, \hat{\theta}_2^{wall})$ circle:*

$$\theta_2 \rightarrow \theta_2 + \Theta_2(e_1, h; q_{1,2}^{wall}) \bmod 2\hat{\theta}_2^{wall}, \quad (25)$$

or, equivalently, to a 2-IEM on the interval $[-\hat{\theta}_2^{wall}, \hat{\theta}_2^{wall}]$ with intervals lengths $\lambda_A = 2\hat{\theta}_2^{wall} - \Theta_2^*, \lambda_B = \Theta_2^*$.

Proof. By lemma 3.5 the flow on level sets belonging to $\mathcal{R}^1(h)$ is topologically conjugated to the $(\omega_1(e_1), \omega_2(h - e_1))$ directional flow on the torus $\mathbb{T}_1(e_1, h - e_1)$ of Eq. (21). Notice that if the level set is in the disallowed region of $\mathcal{R}^1(h)$, then $\hat{\theta}_2^{wall} = \emptyset$, hence $\mathbb{T}_1(e_1, h - e_1) = \emptyset$, so the Theorem trivially holds. For the non-trivial case, by (14), the transverse section Σ_1 to the flow is mapped, for a fixed level set, to the transverse section $\theta_1 = 0$ of the corresponding torus. Hence, to complete the proof we need to show that the return map to the section $\theta_1 = 0$ of the $(\omega_1(e_1), \omega_2(h - e_1))$ directional flow on $\mathbb{T}_1(e_1, e_2)$ is the rotation (25). Indeed, notice that for the level sets in $\mathcal{R}^1(h)$ the effective impact angle is $\hat{\theta}_1^{wall} = \pi$ (when motion is allowed), so $\Theta_2 = \Theta_2^{smooth}(e_1, h) = 2\pi \frac{\omega_2(h-e_1)}{\omega_1(e_1)}$ and thus (25) coincides with the return map on the $\mathbb{T}_1(e_1, h - e_1)$ torus. Similarly, by lemma 3.5, the flow on level sets belonging to $\mathcal{R}^2(h)$ is topologically conjugated to the $(\omega_1(e_1), \omega_2(h - e_1))$ directional flow on the rotated torus $\mathbb{T}_2(e_1, e_2)$ of Eq. (21), namely on $\mathbb{T}_2(e_1, e_2) = \{(\theta_1, \theta_2) | \theta_1 \in [-\hat{\theta}_1^{wall}, \hat{\theta}_1^{wall}), \theta_2 \in [-\pi, \pi)\}$. The return map to the section $\theta_1 = 0$ on this torus is a rotation of the θ_2 angle on the 2π circle by $\omega_2(h - e_1) \frac{2\hat{\theta}_1^{wall}}{\omega_1(e_1)}$, which is exactly Θ_2 (see Eq. (23)). Finally, since $\hat{\theta}_2^{wall} = \pi$ for the allowed level sets in $\mathcal{R}^2(h)$, (25) is verified. \square

Next, we establish that for level sets in $\mathcal{R}^c(h)$, the return map defines a three-interval map on the circle, namely a 5-IEM on the fundamental segment arises. Let

$$\chi_2(e_1, h; q_{1,2}^{wall}) = \frac{\Theta_2^{smooth} - \Theta_2}{2\hat{\theta}_2^{wall}} = \frac{T_1(e_1) - \tilde{T}_1(e_1; q_1^{wall})}{\tilde{T}_2(h - e_1; q_2^{wall})} = \frac{\omega_2(h - e_1)}{\omega_1(e_1)} \frac{\pi - \theta_1^{wall}(e_1; q_1^{wall})}{\theta_2^{wall}(h - e_1; q_2^{wall})} \quad (26)$$

denote the ratio between the time spent above the step and the return time to the upper step boundary. The integer part of χ_2 corresponds to the minimal number of impacts with the upper

boundary of the step during this passage:

$$K_2(e_1, h; q_{1,2}^{wall}) = \lfloor \chi_2 \rfloor. \quad (27)$$

Theorem 4.2. *Under the same conditions of Theorem 2.1, for all iso-energy level sets in $\mathcal{R}^c(h)$, the return map $F_{(e_1, h-e_1)}$ to the section Σ_1 is topologically conjugated to a 3 interval IEM on the θ_2 circle of the form:*

$$(J_R, J_{K_2}, J_{K_2+1}) \rightarrow \Theta_2 + (J_R, J_{K_2+1}, J_{K_2}) \bmod 2\pi, \quad (28)$$

where the lengths of the intervals are:

$$(\lambda_{J_R}, \lambda_{J_{K_2}}, \lambda_{J_{K_2+1}}) = (2\pi - 2\theta_2^{wall}, 2\theta_2^{wall}(1 - \{\chi_2\}), 2\theta_2^{wall}\{\chi_2\}), \quad (29)$$

and the phase of the left boundary of J_R is

$$\theta_{J_R}^L = \theta_2^{wall} - \frac{1}{2}\Theta_2 \bmod 2\pi. \quad (30)$$

In the above formulae $(\theta_2^{wall} = \theta_2^{wall}(h - e_1; q_2^{wall}), \Theta_2, \chi_2)$ are defined by Eqs. (7, 23, 26) respectively and the phase θ_2 is set by (14). The return time to Σ_1 for $\theta_2 \in J_R$ is \tilde{T}_1 whereas for $\theta_2 \in J_{K_2} \cup J_{K_2+1}$ it is T_1 . Equivalently, the dynamics for each level set is conjugated to the induced 5-IEM on the $[-\pi, \pi)$ interval of θ_2 values. This 5-IEM is uniquely defined by Eqs. (28-30), and apart of isolated points of e_1 values in $\mathcal{R}^c(h)$, all its 5 intervals are of positive lengths.

Proof. By lemma 3.6 the flow on level sets belonging to $\mathcal{R}^c(h)$ is topologically conjugated to the $(\omega_1(e_1), \omega_2(h - e_1))$ directional flow on SW - the swiss-cross surface defined by $\theta_1^{wall}(e_1; q_1^{wall})$ and $\theta_2^{wall}(h - e_1; q_2^{wall})$. In particular, the section Σ_1 of the return map is mapped by the action-angle conjugation to the vertical center of SW, the 2π circle of θ_2 phases (see Fig. 8), so the return map on SW and the step dynamics return map to Σ_1 are smoothly conjugated. While the return map can be computed from the SW geometry alone, we find it convenient at times to consider the step dynamics.

We divide the θ_2 circle to two sub-intervals: J_R consisting of phases with trajectories which hit the right boundary of the step (equivalently, the right boundary of the vertical arm of SW) and return to Σ_1 , and J_U consisting of phases with trajectories which do not hit the right boundary (equivalently, enter the horizontal arm of the SW), go above the step, possibly hitting the upper boundary of the step (equivalently, the horizontal boundaries of the SW horizontal arm), and then return to Σ_1 (see Fig. 3 and Fig. 8 where the return map construction to Σ_1 in the configuration space and in the directional flow on the swiss-crossed shaped polygon are shown). Hence, the

length of J_R is the length of the vertical right boundary of the SW, $\lambda_{J_R} = 2\pi - 2\theta_2^{wall} = 2\pi(1 - \frac{\tilde{T}_2}{T_2})$ and $\lambda_{J_U} = 2\theta_2^{wall}$.

The return time for trajectories belonging to J_R is \tilde{T}_1 , the phase θ_2 for these trajectories increases at the constant speed $\omega_2(h - e_1)$, so, the interval J_R is rotated by $2\frac{\omega_2(h-e_1)}{\omega_1(e_1)}\theta_1^{wall}$, namely by Θ_2 as defined in (23).

The return time for trajectories belonging to J_U is T_1 . It is divided to the time \tilde{T}_1 , where the trajectories are to the right of the step and to the time interval $T_1(e_1) - \tilde{T}_1(e_1; q_1^{wall})$ where the trajectories are above the step, possibly bouncing off its upper boundary. During the \tilde{T}_1 time segment the phase θ_2 increases, as before, by Θ_2 . During the $T_1(e_1) - \tilde{T}_1(e_1; q_1^{wall})$ segment, the phase gain depends on the number of bounces. Denote the interval of θ_2 values for which trajectories hit the upper step k times by J_k . The function χ_2 (see Eq. (26)) provides the ratio between the time trajectories in J_U spend above the step and the return time of trajectories with energy $e_2 = h - e_1$ to the step upper boundary. Hence, the number of bounces of the trajectories belonging to J_U is either $K_2 = \lfloor \chi_2 \rfloor$ or $K_2 + 1$, namely, $J_U = J_{K_2} \cup J_{K_2+1}$.

The phase gained during the $T_1(e_1) - \tilde{T}_1(e_1; q_1^{wall})$ segment by trajectories in J_k is $2(\pi - \theta_2^{wall})k + \omega_2\tilde{T}_2\chi_u = 2(\pi - \theta_2^{wall})k + 2\theta_2^{wall}(\lfloor \chi_2 \rfloor + \{\chi_2\}) = 2\pi k + 2\theta_2^{wall}(K_2 - k) + 2\theta_2^{wall}\{\chi_u\}$, hence, applying this formula for $k = K_2$ and for $k = K_2 + 1$ we obtain:

$$F(\theta_2) = \begin{cases} \theta_2 + \Theta_2 & \theta_2 \in J_R \\ \theta_2 + \Theta_2 + 2\theta_2^{wall}\{\chi_2\} + 2\pi K_2 & \theta_2 \in J_{K_2} \\ \theta_2 + \Theta_2 + 2\theta_2^{wall}(-1 + \{\chi_2\}) + 2\pi(K_2 + 1) & \theta_2 \in J_{K_2+1} \end{cases} \quad (31)$$

where the intervals $(J_R, J_{K_2}, J_{K_2+1})$, correspond, respectively, to phases with trajectory segments which hit exactly once only the right side of the step (J_R), those which hit only the upper side of the step exactly K_2 times (J_{K_2}) and those hitting only the upper side exactly $K_2 + 1$ times (J_{K_2+1}), where $K = K_2(e_1, h)$ (see eq. (26-27)). Notice that χ_2 is finite since $\tilde{T}_2 > 0$ for level sets in the step region (yet, χ_2 diverges at the step-region boundary when $q_2^{wall} > 0$, see Table 2).

The order of these intervals on the circle is $(J_R, J_{K_2}, J_{K_2+1})$; this follows from the geometry of the swiss-crossed surface or from realizing that the right (resp. left) most end point of J_R corresponds to a trajectory which hits the corner with positive (resp. negative) vertical velocity, hence, a small shift into the interval J_U will result in missing the step on the right side and hitting the upper part of the step on the left side, see Figure 11.

Under the return map to Σ_1 the two intervals J_{K_2}, J_{K_2+1} switch their position and J_U and J_R rotate by Θ_2 ; This follows from formulae (31). Indeed, the dividing trajectory between these two intervals is the trajectory that hits the corner from the direction above the step (i.e. with

$p_1 > 0, p_2 < 0$), and this dividing trajectory is glued to the lower boundary of J'_R - since the return map is piece-wise orientation preserving this implies that J_{K_2}, J_{K_2+1} must switch their positions - see Figure 11. In summary, we proved Eq. (28).

The lengths of the intervals, λ_α of Eq. (29), follow either from the swiss-cross geometry, or, equivalently, from formulae (31), or by considering the phases of the trajectories which hit the step corner (see Fig. 11):

$$\lambda_{J_{K_2+1}} = 2\pi \frac{\tilde{T}_2}{T_2} \left\{ \frac{T_1 - \tilde{T}_1}{\tilde{T}_2} \right\} = 2\theta_2^{wall} \{\chi_2\} \quad (32)$$

$$\lambda_{J_{K_2}} = 2\pi \frac{\tilde{T}_2}{T_2} \left(1 - \left\{ \frac{T_1 - \tilde{T}_1}{\tilde{T}_2} \right\} \right) = 2\theta_2^{wall} (1 - \{\chi_2\})$$

The form of the IEM on the circle is now fully determined by the rotation (23), the permutation (28), and the lengths of the intervals (29).

To determine the 5-IEM on the fundamental interval $[-\pi, \pi)$, we need to identify how the circle-intervals and their images J_α, J'_α , are cut by the chosen fundamental interval, here $[-\pi, \pi)$. Let $\theta_{J_\alpha}^{L,R}, \theta_{J'_\alpha}^{L,R} \in [-\pi, \pi)$ denote the left and right end points of the circle interval $J_\alpha, J'_\alpha \bmod 2\pi$. Namely, when $\theta_{J_\alpha}^L < \theta_{J'_\alpha}^R$ the circle interval J_α is not cut by the fundamental interval, so $J_\alpha^* = [\theta_{J_\alpha}^L, \theta_{J'_\alpha}^R) \subset [-\pi, \pi)$ whereas $\theta_{J_\alpha}^L > \theta_{J'_\alpha}^R$ means that J_α is split to two intervals, so: $J_\alpha^* = J_\alpha^1 \cup J_\alpha^2 = [-\pi, \theta_{J'_\alpha}^R) \cup [\theta_{J_\alpha}^L, \pi)$, and the same convention is applied to the intervals images. To obtain the 5-IEM, given an α such that $\theta_{J_\alpha}^L > \theta_{J'_\alpha}^R$ we split that interval to two at the phase π . Similarly, given an α such that $\theta_{J'_\alpha}^L > \theta_{J_\alpha}^R$ we split its pre-image, J_α at θ^* - the pre-image of π . In the non-degenerate case (i.e. when $\theta_{J_\alpha}^{L,R}, \theta_{J'_\alpha}^{L,R} \neq -\pi, J_\alpha \in \{J_R, J_{K_2}, J_{K_2+1}\}$), exactly one of the intervals and exactly one image of an interval is split, so, if additionally $\{\chi_2\} \neq 0$, we obtain a 5-IEM. We identify below the J_R interval end points and their images and demonstrate that this completely determines the 5-IEM on $[-\pi, \pi)$.

The left boundary of J_R , $\theta_{J_R}^L$, is the phase of the trajectory which reaches the corner from the right with negative vertical velocity, i.e. it is the phase on Σ_1 which arrives to the corner $(\theta_1^{wall}, \theta_2^{wall})$ in the swiss cross (see Figure 11). Since the time of passage from Σ_1 to Σ_1^- is half of \tilde{T}_1 , and since the phases in J_R are rotated by the phase Θ_2 , we immediately obtain that :

$$\theta_{J_R}^L = \theta_{J_{K_2+1}}^R = \theta_2^{wall} - \frac{1}{2}\Theta_2 \pmod{2\pi}, \quad \theta_{J_R}^L = \theta_{J_{K_2}}^R = \theta_2^{wall} + \frac{1}{2}\Theta_2 \pmod{2\pi}. \quad (33)$$

This information, together with the order of the intervals (28) and their lengths (29) completely

determines the 5 IEM. Indeed,

$$\theta_{J_R}^R = \theta_{J_{K_2}}^L = \theta_{J_R}^L + \lambda_{J_R} \pmod{2\pi}, \quad (34)$$

hence

$$\theta_{J_{K_2+1}}^L = \theta_{J_R}^R = \theta_{J_R}^L + \Theta_2 \pmod{2\pi}, \quad (35)$$

and,

$$\theta_{J_{K_2}}^R = \theta_{J_{K_2+1}}^L = \theta_{J_{K_2}}^L + \lambda_{J_{K_2}} \pmod{2\pi}, \quad (36)$$

so,

$$\theta_{J_{K_2}}^L = \theta_{J_{K_2+1}}^R = \theta_{J_{K_2+1}}^L + \lambda_{J_{K_2+1}} \pmod{2\pi}, \quad (37)$$

and all the intervals' and their images' end points are thus determined by $\chi_2, \Theta_2, \theta_2^{wall}$ (all depending on (e_1, h) and on the parameters e.g. $q_{1,2}^{wall}$). In particular, the conditions under which one or more of the 5-intervals in $[-\pi, \pi)$ has zero length can be explicitly formulated:

$$\Theta_2(e_1, h, q_1^{wall}) = \begin{cases} \Theta^{smooth}(e_1, h) - 2K\theta_2^{wall}(h - e_1, q_2^{wall}) & \text{then } \lambda_{J_{K+1}} = 0 \\ \pm 2\theta_2^{wall}(h - e_1, q_2^{wall}) + 2\pi(1 + 2M) & \text{then } -\pi \in \{\theta_{J_R}^{L,R}, \theta_{J_R'}^{L,R}\} \\ 2\theta_2^{wall}(h - e_1, q_2^{wall})(1 - 2\{\chi_u\}) + 2\pi(1 + 2M) & \text{then } -\pi \in \{\theta_{J_K}^R, \theta_{J_{K+1}}^R\} \end{cases} \quad (38)$$

where $K, M \in \mathbb{Z}$. To complete the proof, we need to show that these conditions may be satisfied at most at isolated e_1 values. To this aim, we first notice:

Lemma 4.3. *For level sets in the step region \mathcal{R}^c , the functions $\chi_2, \Theta_2, \theta_2^{wall}$ of e_1 are pair-wise independent, and, when Θ_2^{smooth} is non-constant, they are also pair-wise independent of Θ_2^{smooth} .*

Corner position	$\chi_2(h_1^{step}), \chi_2(h - h_2^{step})$	$\Theta_2(h_1^{step}), \Theta_2(h - h_2^{step})$
$q_{1,2}^{wall} < 0$	$0, \frac{\Theta_2^{smooth}(h-h_2^{step})(1-\frac{\theta_1^{wall}(h-h_2^{step})}{\pi})}{2\pi}$	$\Theta_2^{smooth}(h_1^{step}, h), \frac{\Theta_2^{smooth}(h-h_2^{step})\theta_1^{wall}(h-h_2^{step})}{\pi}$
$q_1^{wall} < 0, q_2^{wall} > 0$	$0, \infty$	$\Theta_2^{smooth}(h_1^{step}, h), \frac{\Theta_2^{smooth}(h-h_2^{step})\theta_1^{wall}(h-h_2^{step})}{\pi}$
$q_1^{wall} > 0, q_2^{wall} < 0$	$\frac{\Theta_2^{smooth}(h_1^{step}, h)}{2\theta_2^{wall}(h-h_1^{step})}, \frac{\Theta_2^{smooth}(h-h_2^{step})(1-\frac{\theta_1^{wall}(h-h_2^{step})}{\pi})}{2\pi}$	$0, \frac{\Theta_2^{smooth}(h-h_2^{step})\theta_1^{wall}(h-h_2^{step})}{\pi}$
$q_{1,2}^{wall} > 0$	$\frac{\Theta_2^{smooth}(h_1^{step}, h)}{2\theta_2^{wall}(h-h_1^{step})}, \infty$	$0, \frac{\Theta_2^{smooth}(h-h_2^{step})\theta_1^{wall}(h-h_2^{step})}{\pi}$

Table 2: The values of χ_2, Θ_2 at the two edges of $\bar{\mathcal{R}}^c(h)$

Proof. The independence follows from the observation that the functions are smooth non-constant functions (see Tables 1,2) that depend non-trivially on e_1 through distinct parameters. For example, $\Theta_2 = \Theta_2(e_1, h, q_1^{wall})$ whereas $\theta_2^{wall} = \theta_2^{wall}(h - e_1, q_2^{wall})$ and the dependence of these two

functions on e_1 through $q_{1,2}^{wall}$ is non-trivial (i.e., it follows from Eq. (7,23) that $\frac{\partial^2 \theta_2^{wall}}{\partial q_2^{wall} \partial e_1} = -\frac{d}{de_1} \frac{\omega_i(e_i)}{\sqrt{2(e_i - V_i(q_i^{wall}))}}$ and $\frac{\partial^2 \Theta_2}{\partial q_1^{wall} \partial e_1} = -\frac{d}{de_1} \frac{2\omega_2(h - e_1)}{\sqrt{2(e_1 - V_1(q_1^{wall}))}}$ hence, with, possibly, the exception of isolated e_1 values, these derivatives do not vanish for all level sets in \mathcal{R}^c). Hence, if they were functionally dependent, i.e. there was a $G(\theta_2^{wall}, \Theta_2; h, q_{1,2}^{wall}) \equiv 0$ then $\frac{d}{dq_2^{wall}} G(\theta_2^{wall}, \Theta_2; h, q_{1,2}^{wall}) = \frac{\partial G}{\partial \theta_2^{wall}} \frac{\partial \theta_2^{wall}}{\partial q_2^{wall}} + \frac{\partial G}{\partial \Theta_2} \frac{\partial \Theta_2}{\partial q_2^{wall}} \equiv 0$ and hence $\frac{d^2}{de_1 dq_2^{wall}} G(\theta_2^{wall}, \Theta_2; h, q_{1,2}^{wall}) = \frac{\partial G}{\partial \theta_2^{wall}} \frac{\partial^2 \theta_2^{wall}}{\partial e_1 \partial q_2^{wall}} + \frac{\partial}{\partial \theta_2^{wall}} \frac{\partial \Theta_2}{\partial q_2^{wall}} + \frac{\partial}{\partial \Theta_2} \frac{\partial \Theta_2}{\partial q_2^{wall}} = \frac{\partial G}{\partial \theta_2^{wall}} \frac{\partial^2 \theta_2^{wall}}{\partial e_1 \partial q_2^{wall}} = 0$. Since $\frac{\partial^2 \theta_2^{wall}}{\partial e_1 \partial q_2^{wall}} \neq 0$ we conclude that $\frac{\partial G}{\partial \theta_2^{wall}} = 0$, namely, there is no such G with non-trivial dependence on both θ_2^{wall} and Θ_2). Similarly, since $\chi_2 = \chi_2(e_1, h, q_1^{wall}, q_2^{wall})$, and similarly to the above calculations, the dependence of χ_2 on both q_1^{wall} and q_2^{wall} is non-trivial in e_1 , the pairs (χ_2, Θ_2) and $(\chi_2, \theta_2^{wall})$ are functionally independent. Finally, since $\Theta_2^{smooth} = \Theta_2^{smooth}(e_1, h)$, by the same argument as above, provided $\frac{\partial \Theta_2^{smooth}(e_1, h)}{\partial e_1} \neq 0$ apart of isolated points, it is pair-wise independent from each of the functions $\chi_2, \Theta_2, \theta_2^{wall}$. \square

Now, we can show that (38) is satisfied at most at isolated e_1 values. For the first two possibilities, both sides of the equation are smooth functions of e_1 with the right hand side depending non-trivially on q_1^{wall} whereas the left hand side depending non-trivially on q_2^{wall} . Hence, by the same arguments as in lemma 4.3, the right and left hand side are functionally independent and their difference vanish at most at isolated e_1 values.

For the last row, notice that

$$\chi_2(e_1, h, q_1^{wall}, q_2^{wall}) = \frac{T_2(h - e_1)}{\tilde{T}_2(h - e_1)} \frac{T_1(e_1) - \tilde{T}_1(e_1)}{T_2(h - e_1)} = \frac{\Theta_2^{smooth} - \Theta_2}{2\theta_2^{wall}}, \quad (39)$$

namely, $2\{\chi_u\}\theta_2^{wall} = \Theta_2^{smooth} - \Theta_2 - 2K_2\theta_2^{wall}$, hence the last equation becomes

$$2\theta_2^{wall}(h - e_1; q_2^{wall})(1 + 2K_2) = 2\Theta_2^{smooth}(e_1, h) - \Theta_2(e_1, h, q_1^{wall}) - 2\pi(1 + 2M), \quad (40)$$

which shows, as above, that it is also satisfied at most at isolated e_1 values.

Notice that $\theta_2^{wall} > 0$ for all level sets in $\mathcal{R}^c(h)$, so the circle map has always at least two non-trivial components (J_R and J_U), and in fact, with the exception of isolated points within $\mathcal{R}^c(h)$, it has three non-trivial components since $\{\chi_2\}$ vanishes at most at isolated e_1 values. \square

5 Additional properties of the family of IEM.

Theorem 4.2 implies that the dynamics for level sets in the step set are completely determined by the numerical properties of $\chi_2, \Theta_2, \theta_2^{wall}$. All these functions depend smoothly on e_1 for the level sets in $\mathcal{R}^c(h)$ and are non-constant functions - indeed, their values at the boundaries of $\mathcal{R}^c(h)$ are

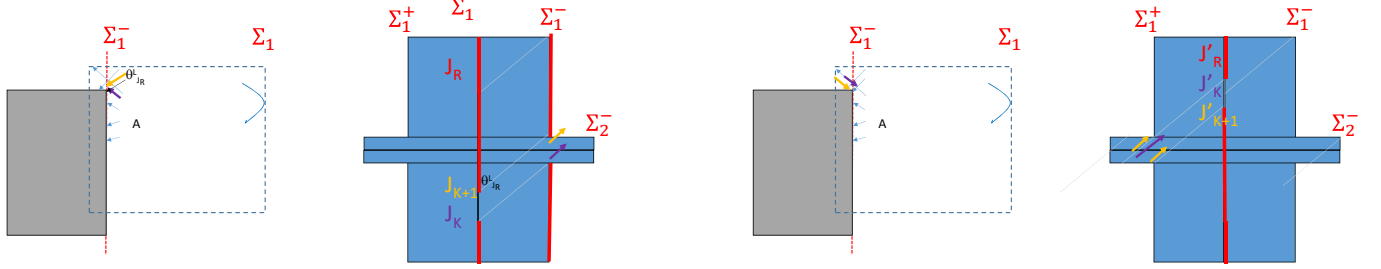


Figure 11: Order of intervals: the intervals J_{K_2}, J_{K_2+1} correspond to orbits that bounce, respectively, $K_2, K_2 + 1$ times above the step. On the SW surface these are the orbits that enter the horizontal arm and wrap, respectively, $K_2, K_2 + 1$ times around it before returning to the vertical arm. Thus, their order on Σ_1 is reversed by the flow (Eq. (11)). The phase $\theta_{J_R}^L$ denotes the left edge of J_R - the phase that separates the orbits that enter the horizontal arm from those that bounce off the vertical arm boundary, namely the vertical boundary of the step.

always distinct - see Tables 1 and 2. Hence, these functions attain both rational and irrational values as e_1 is varied (in some cases, but not all, these functions are also monotone in e_1). While one may suspect that this implies that for almost all e_1 values the dynamics are uniquely ergodic, it is difficult to check directly when the corresponding IEM satisfies the Veech condition (see [11]). Indeed, while Lemma 4.3 states that the functions $\chi_2, \Theta_2, \theta_2^{wall}$ are pair-wise independent, and, in Theorem 4.2 we established that the lengths of the intervals of the IEM are non-zero with the exception of isolated e_1 values, more delicate relations between the intervals lengths may arise. Indeed, rewriting Eq. (39) as:

$$\Theta_2^{smooth}(e_1, h) = 2\theta_2^{wall}(h - e_1, q_2^{wall})\chi_2(e_1, h, q_1^{wall}, q_2^{wall}) + \Theta_2(e_1, h, q_1^{wall}), \quad (41)$$

shows that in the linear case, where $\Theta_2^{smooth, LO} = 2\pi \frac{\omega_2}{\omega_1}$, the three functions are functionally related! The implications of this dependence on the dynamics and the properties of it for general nonlinear oscillators are yet to be explored. For now we show, by analyzing the properties of these functions, that, for some cases minimal dynamics arise and in others non-minimal dynamics arise.

In particular, we establish that there can be isolated strongly resonant level sets at which orbits of different periods co-exist (e.g. if $\frac{\Theta_2}{2\pi}, \frac{2\theta_2^{wall}}{2\pi}, \{\chi_2\} \in \mathbb{Q}$), level sets for which periodic and quasi-periodic motion co-exist (e.g. when $\{\frac{\Theta}{2\pi}, \frac{2\theta_2}{2\pi}\} \in \mathbb{Q}, \{\chi_2\} \notin \mathbb{Q}$ such a case may emerge) and

isolated level sets in $\mathcal{R}^c(h)$ at which the IEM reduces to a rotation (when $\{\chi_2\} = 0$ so the directional flow on SW has a diagonal trajectory in the horizontal arm). Notice that the analogous computations for the return map to Σ_2 amounts to replacing $1 \leftrightarrow 2$ in all the above definitions.

In particular, we notice the special role the function χ_2 plays: its magnitude controls the number of bounces experienced by phases in J_{K_2} (recall that $K_2 = \lfloor \chi_2 \rfloor$) and its phase, $\{\chi_2\}$, controls the division of J_U to two intervals (recall that $\lambda_{J_{K_2+1}} = 2\theta_2^{wall}\{\chi_2\}$). Hence, we study the dependence of χ_2 on e_1 and on the parameters $q_{1,2}^{wall}$. We begin with two simple cases where we can completely characterize the dynamics:

Corollary 5.1. *For level sets in $\mathcal{R}^c(h)$ for which $\{\chi_2\} = 0$ the return map to Σ_1 is of only 2 intervals, namely it corresponds to a rotation by Θ_2 , and is thus ergodic iff $\Theta_2/2\pi \notin \mathbb{Q}$.*

Proof. By (29), $\{\chi_2\} = 0$ implies that $\lambda_{J_{K_2}} = 2\theta_2^{wall} > 0$ and $\lambda_{J_{K_2+1}} = 0$, hence, (31) becomes a rotation by Θ_2 . \square

In terms of the directed motion on the L-shaped billiard, the condition $\{\chi_2\} = 0$ corresponds to the case of a diagonal orbit connecting the corners of the horizontal arm. If, additionally, $\Theta_2/2\pi \in \mathbb{Q}$ then this orbit is also a diagonal of the vertical arm. Notably, if $q_2^{wall} > 0$, close to the boundary of $\mathcal{R}^c(h)$ the horizontal sleeve becomes narrow (see Fig. 12) and thus there are many level sets at which $\{\chi_2\} = 0$:

Lemma 5.2. *If $q_2^{wall} > 0$, for all $h > h^{step}$, there are countable infinite level sets in $\mathcal{R}^c(h)$ for which $\{\chi_2\} = 0$.*

Proof. Since, for $q_2^{wall} > 0$, $\tilde{T}_2(h - e_1; q_2^{wall}) \rightarrow 0$ as $e_1 \rightarrow h - h_2^{step}$ whereas $T_1(e_1) - \tilde{T}_1(e_1; q_1^{wall})$ attains a finite positive limit (since $h > h^{step}$), the smooth function $\chi_2(e_1, h) = \frac{T_1(e_1) - \tilde{T}_1(e_1)}{\tilde{T}_2(h - e_1)}$ in the open interval $\mathcal{I}^c(h)$ becomes infinite on the interval right boundary, hence it passes through integer values at countable infinite values of e_1 . \square

Another case which allows a complete characterization of the motion is when Θ_2 is rational and θ_2^{wall} is small:

Lemma 5.3. *For level sets in $\mathcal{R}^c(h)$ for which $\Theta_2 = \frac{2\pi m}{n}$ and $2\theta_2^{wall} < \frac{2\pi}{n}$, the IEM to Σ_1 is non-ergodic. For such level sets, if $\{\chi_u\} \notin \mathbb{Q}$ the motion is dense on a union of open intervals and is periodic on its complement. If $\{\chi_u\} \in \mathbb{Q}$, all i.c. are periodic, yet, there are two distinct periods. All the above conditions are realizable for some level sets and wall positions.*

Proof. Let $I = [-\pi, \pi) \setminus \bigcup_{j=0}^{n-1} F^j(J_U) \subset J_R$ where $J_U = J_{K_2} \cup J_{K_2+1}$. Since here $\lambda_{J_U} = 2\theta_2^{wall} < \frac{2\pi}{n}$, this is a non-empty set. It is invariant since the end points of J_U belong to J_R , so the end points are n -periodic. Hence, all the i.c. in I are n periodic and thus F is non-ergodic on the circle.

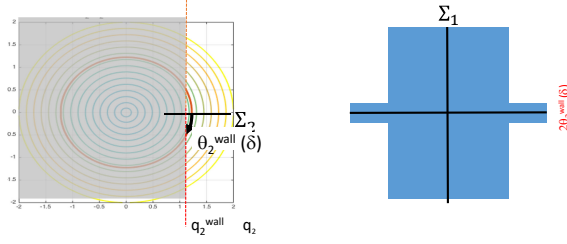


Figure 12: The dynamics for small θ_2^{wall} .

The dynamics in the complement to I , namely the invariant set $\bigcup_{j=0}^{n-1} F^j(J_U)$, depends on the numerical value of $\{\chi_2\}$. Notice that for all i.c. in J_{K_2} , $F^n(\theta_2) = \theta_2 + 2\theta_2^{wall} \{\chi_u\} \in J_U$ whereas for all i.c. in J_{K_2+1} , $F^n(\theta_2) = \theta_2 - 2\theta_2^{wall}(1 - \{\chi_u\}) \in J_U$, namely, $F^n(\theta_2)$ is a 2-IEM on J_U , hence it is periodic for $\{\chi_u\} = \frac{p}{q} \in \mathbb{Q}$ and is dense in J_U otherwise. In the periodic case, initial conditions in I are n -periodic whereas initial conditions in its complement are nq periodic. Finally, since the functions $\Theta_2, \chi_2, \theta_2^{wall}$ are continuous (in fact, smooth) non-constant functions of e_1 in $\mathcal{I}^c(h)$ and since $\Theta_2 = \Theta_2(e_1, h, q_1^{wall})$ we obtain that for every h, q_1^{wall} there is a countable set of e_1 values in $\mathcal{I}^c(h)$, $e_1^* = e_1(\frac{m}{n}, h, q_1^{wall})$ for which $\Theta_2 = \frac{2\pi m}{n}$. Notice that Θ_2 does not depend explicitly on q_2^{wall} . Fixing $\frac{m}{n}, h, q_1^{wall}$, there is a $q_2^{wall}(\delta)$ value such that $2\theta_2^{wall}(h - e_1^*, q_2^{wall}) < \frac{2\pi}{n}$ for all $q_2^{wall} > q_2^{wall}(\delta)$; indeed, choose $q_2^{wall}(\delta) > 0$ such that $V_2(q_2^{wall}(\delta)) = h - e_1^* - \delta$, so, by (7) and (18), for small δ , $\theta_2^{wall}(\delta) = \theta_2^{wall}(h - e_1^*, q_2^{wall}(\delta))$ is monotone decreasing (in δ) to 0 (see Fig. 12). In particular, there exists $\delta^*(n)$ such that for all $\delta \in (c\delta^*(n), \delta^*(n))$, for any $0 < c < 1$, the impact angle satisfies $2\theta_2^{wall}(c\delta^*(n)) < 2\theta_2^{wall}(\delta) < \frac{2\pi}{n}$, so it is small yet bounded away from 0, as needed for the smooth dependence on e_1 near e_1^* . In particular, for this range of $q_2^{wall}(\delta)$ values, motion on the level set $(e_1^*, h - e_1^*)$ is n -periodic for the set I as described above. Moreover, on this level set, from (26), $\chi_2(\delta) = \frac{\Theta^{smooth}(e_1^*, h) - \frac{2\pi m}{n}}{\theta_2^{wall}(\delta)} > 0$, hence, it is a continuous monotone increasing function of δ , and thus, $\{\chi_u\} \notin \mathbb{Q}$ for almost all δ values in the interval and there is a countable set of δ values for which $\{\chi_u\} \in \mathbb{Q}$. Namely, we established that these conditions are always realizable by varying the parameter q_2^{wall} . \square

Notice that for sufficiently small c in the above proof the function $\chi_2(\delta)$ becomes large, as in lemma 5.2, therefore, $\{\chi_2(\delta)\}$ vanishes at some isolated δ values. Finally, since χ_2 is continuous, its range for $e_1 \in \mathcal{I}^c(h)$ is at least as large as the interval $(\chi_2(h_1^{step}), \chi_2(h - h_2^{step}))$. When one of these values is an integer, the behavior below and above this energy changes. Thus, Table 2

provides conditions for energy values at which bifurcations occur. For linear oscillators, we can find the ranges explicitly, see section 6.

All the above properties were stated for the return map to Σ_1 , creating an artificial asymmetry between the horizontal and vertical directions. The same results apply to the return map to the Σ_2 section by reversing the roles of 1 and 2 and horizontal and vertical in all definitions.

6 The step dynamics for linear oscillators

For the quadratic potentials (Eq. (2)), the L-shaped billiard tables vertices are found explicitly and the direction of motion is fixed. We begin this section by proving Theorems 2.5 regarding the linear-oscillators-step dynamics and continue with additional observations regarding the singular level sets for this case.

Proof. of Theorem 2.5: The transformation to action angle coordinates for linear oscillators, with the convention (14), becomes: $(q_i(t), p_i(t)) = (\sqrt{\frac{2I_i}{\omega_i}} \cos \theta_i(t), -\sqrt{2I_i\omega_i} \sin \theta_i(t))$, $H_i = \omega_i I_i$, and $I_i = \frac{1}{2}(\frac{p_i^2}{\omega_i} + \omega_i q_i^2)$. Hence, for $e_i > h_i^{step} = \frac{1}{2}\omega_i^2(q_i^{wall})^2$:

$$\theta_i^{wall, LO}(e_i; q_i^{wall}) = \arccos \sqrt{\frac{\omega_i}{2I_i}} q_i^{wall} = \arccos \frac{\omega_i q_i^{wall}}{\sqrt{2e_i}} \in \begin{cases} (\frac{\pi}{2}, \pi) & q_i^{wall} < 0 \\ (0, \frac{\pi}{2}) & q_i^{wall} > 0. \end{cases} \quad (42)$$

Since the frequencies of linear oscillators are independent of the energy, the direction of motion in the iso-energetic billiard family, $\mathcal{B}(h)$, is fixed to (ω_1, ω_2) for all the level sets. Hence, for a given energy surface $h = e_1 + e_2 > h^{step}$, the linear oscillator step dynamics on each level set $(e_1, e_2 = h - e_1) \in \mathcal{R}^c(h)$ are conjugated to the directed billiard motion, in direction (ω_1, ω_2) , in the L-shaped billiards $L(\pi, \pi, \arccos \frac{\omega_1 q_1^{wall}}{\sqrt{2e_1}}, \arccos \frac{\omega_2 q_2^{wall}}{\sqrt{2(h-e_1)}})$. Moreover, since

$$\frac{d\theta_1^{wall, LO}(e_1; q_1^{wall})}{de_1} = \frac{\omega_1 q_1^{wall}}{2e_1} \frac{1}{\sqrt{2e_1 - (\omega_1 q_1^{wall})^2}} \quad (43)$$

and

$$\frac{d\theta_2^{wall, LO}(h - e_1; q_1^{wall})}{de_1} = -\frac{\omega_2 q_2^{wall}}{2(h - e_1)} \frac{1}{\sqrt{2(h - e_1) - (\omega_2 q_2^{wall})^2}}, \quad (44)$$

the widths of the arms are monotone in e_1 and are of opposite monotonicity iff $q_1^{wall} q_2^{wall} > 0$.

□

As shown in section 5, the monotonicity, bounds and limits of the functions $\Theta_2, \chi_2, \theta_2^{wall}$ determine the variety of behaviors of the dynamics on iso-energy surfaces. For linear oscillators, $\Theta_2^{LO}, \theta_2^{wall, LO}$ are monotone in the step region whereas:

Lemma 6.1. *For all $h > h^{step}$, the function $\chi_2^{LO}(e_1, h)$ is monotone iff $q_1^{wall} q_2^{wall} < 0$.*

Proof. Observe that for linear oscillators $q_i^{wall} \tilde{T}_i^{LO}(e_i; q_i^{wall}) > 0$ (see Eqs. (7,9) and recall that $T_i^{LO} = 0$, hence the result follows from the definition (26) of $\chi_2(e_1, h)$, or, from direct differentiation

$$\text{of } \chi_2^{LO}(e_1, h) = \frac{\omega_2}{\omega_1} \frac{(\pi - \arccos \frac{\omega_1 q_1^{wall}}{\sqrt{2e_1}})}{\arccos \frac{\omega_2 q_2^{wall}}{\sqrt{2(h-e_1)}}} = \frac{\omega_2}{\omega_1} \frac{\pi - \theta_1^{wall, LO}(e_1; q_1^{wall})}{\theta_2^{wall, LO}(h-e_1; q_2^{wall})} \text{ (see (11))}:$$

$$\chi_2^{LO'}(e_1) = \frac{\omega_2 \left(-\frac{\omega_1 q_1^{wall} \arccos \frac{\omega_2 q_2^{wall}}{\sqrt{2(h-e_1)}}}{2e_1 \sqrt{2e_1 - (\omega_1 q_1^{wall})^2}} + \frac{\omega_2 q_2^{wall} (\pi - \arccos \frac{\omega_1 q_1^{wall}}{\sqrt{2e_1}})}{2(h-e_1) \sqrt{2(h-e_1) - (\omega_2 q_2^{wall})^2}} \right)}{\omega_1 (\arccos \frac{\omega_2 q_2^{wall}}{\sqrt{2(h-e_1)}})^2}. \quad (45)$$

The denominator is always positive (it approaches 0 when $q_2^{wall} > 0$ and $e_1 \nearrow h - \frac{1}{2}(\omega_2 q_2^{wall})^2$) so the sign is determined by the numerator. If $q_1^{wall} q_2^{wall} < 0$ both terms in the numerator have the same sign so χ_2 is monotone. If $q_1^{wall} q_2^{wall} > 0$, the first term in the numerator diverges to $-sign(q_1^{wall})\infty$ as $e_1 \searrow \frac{1}{2}(\omega_1 q_1^{wall})^2$, the second term diverges to $sign(q_2^{wall})\infty$ as $e_1 \nearrow h - \frac{1}{2}(\omega_2 q_2^{wall})^2$, hence $\chi_2'(e_1)$ changes sign and χ_2 is non-monotone. \square

Corollary 6.2. *If $q_2^{wall} > 0$, for all $h > h^{step}$, the step region has countable infinite level sets at which $\{\chi_2^{LO}\} = 0$, namely at which the return map to Σ_1 reduces to a two intervals rotation on the circle. For $q_2^{wall} < 0$, for sufficiently large h , the number, $N_{osc}^2(h)$, of such level sets when $q_1^{wall} < 0$ is at least $\left\lfloor \frac{1}{2} \frac{\omega_2}{\omega_1} \right\rfloor$ whereas if $q_1^{wall} > 0$ there are $\left\lfloor \frac{3}{2} \frac{\omega_2}{\omega_1} \right\rfloor$ such level sets. The same results hold for the return map to Σ_2 when replacing the roles of $1 \leftrightarrow 2$ in the above statements.*

Proof. First, it follows from (11) that in the step region $\chi_2^{LO}(e_1, h)$ is a smooth non-oscillatory function which diverges only at the step region upper boundary (and this occurs iff $q_2^{wall} > 0$). Hence, for any fixed h , there is at most countable infinite level sets $N_{osc}^2(h)$ at which $\{\chi_2^{LO}(e_1)\}$ may vanish. The edge values - the values of $\chi_2^{LO}, \Theta_2^{LO}$ at the end points of the step-region (namely calculating (9),(11) at $e_1 = h_1^{step}$ and at $e_1 = h - h_2^{step}$) and their monotonicity property are listed in Table 3, where

$$\theta_1^*(h) = \theta_1^{wall}(h - h_2^{step}; q_1^{wall}) = \arccos \frac{\omega_1 q_1^{wall}}{\sqrt{2h - (\omega_2 q_2^{wall})^2}} \quad (46)$$

$$\theta_2^*(h) = \theta_2^{wall}(h - h_1^{step}; q_2^{wall}) = \arccos \frac{\omega_2 q_2^{wall}}{\sqrt{2h - (\omega_1 q_1^{wall})^2}}. \quad (47)$$

Corner position	$\chi_2^{LO}(h_1^{step}) \rightarrow \chi_2^{LO}(h - h_2^{step})$	$\Theta_2^{LO}(h_1^{step}) \rightarrow \Theta_2^{LO}(h - h_2^{step})$
$q_{1,2}^{wall} < 0$	$0 \nearrow \searrow \frac{\omega_2(1 - \frac{1}{\pi}\theta_1^*(h))}{\omega_1}$	$2\pi \frac{\omega_2}{\omega_1} \searrow 2\frac{\omega_2}{\omega_1}\theta_1^*(h)$
$q_1^{wall} < 0, q_2^{wall} > 0$	$0 \nearrow \infty$	$2\pi \frac{\omega_2}{\omega_1} \searrow 2\frac{\omega_2}{\omega_1}\theta_1^*(h)$
$q_1^{wall} > 0, q_2^{wall} < 0$	$\frac{\omega_2}{\omega_1} \frac{\pi}{\theta_2^*(h)} \searrow \frac{\omega_2(1 - \frac{1}{\pi}\theta_1^*(h))}{\omega_1}$	$0 \nearrow 2\frac{\omega_2}{\omega_1}\theta_1^*(h)$
$q_{1,2}^{wall} > 0$	$\frac{\omega_2}{\omega_1} \frac{\pi}{\theta_2^*(h)} \searrow \nearrow \infty$	$0 \nearrow 2\frac{\omega_2}{\omega_1}\theta_1^*(h)$

Table 3: The values of $\chi_2^{LO}, \Theta_2^{LO}$ at the edges of $\mathcal{R}^c(h)$ and their monotonicity properties.

For any energy h , these values supply the range of χ_2^{LO} in the monotone cases (second and third rows in the tables) and a lower bound on its range in the non-monotone cases (first and last rows). The number of iso-energy level sets at which $\{\chi_2^{LO} = 0\}$ (at which the directional motion in the horizontal arm of the SW surface is diagonal) is determined by the number of integer values contained in the range of χ_2^{LO} . The second and fourth rows of Table 3 show that the range is infinite when $q_2^{wall} > 0$, proving the first statement of the corollary. Table 4 shows the asymptotic edge values at large energies, using the observation that $\theta_{1,2}^*(h) \rightarrow \frac{\pi}{2}$. The rest of the corollary follows from this table - for $q_2^{wall} < 0$, the first row of Tables 4 corresponds to the non-monotone case whereas the third row corresponds to the monotone case. Since $N_{osc}^2(h)$ are integers, for sufficiently large h the limiting values and $N_{osc}^2(h)$ are identical. Finally, by symmetry, replacing the roles of $1 \leftrightarrow 2$, provides the estimates for $N_{osc}^1(h)$, the number of oscillations in the vertical arm before returning to the section Σ_2 .

Corner position	χ_2^{LO}	Θ_2^{LO}	N_{osc}^2	N_{osc}^1
$q_{1,2}^{wall} < 0$	$0 \nearrow \searrow \frac{\omega_2}{2\omega_1}$	$2\pi \frac{\omega_2}{\omega_1} \searrow \pi \frac{\omega_2}{\omega_1}$	$\geq \lfloor \frac{1}{2} \frac{\omega_2}{\omega_1} \rfloor$	$\geq \lfloor \frac{1}{2} \frac{\omega_1}{\omega_2} \rfloor$
$q_1^{wall} < 0, q_2^{wall} > 0$	$0 \nearrow \infty$	$2\pi \frac{\omega_2}{\omega_1} \searrow \pi \frac{\omega_2}{\omega_1}$	∞	$\lfloor \frac{3}{2} \frac{\omega_1}{\omega_2} \rfloor$
$q_1^{wall} > 0, q_2^{wall} < 0$	$\frac{2\omega_2}{\omega_1} \searrow \frac{\omega_2}{2\omega_1}$	$0 \nearrow \pi \frac{\omega_2}{\omega_1}$	$\lfloor \frac{3}{2} \frac{\omega_2}{\omega_1} \rfloor$	∞
$q_{1,2}^{wall} > 0$	$\frac{2\omega_2}{\omega_1} \searrow \nearrow \infty$	$0 \nearrow \pi \frac{\omega_2}{\omega_1}$	∞	∞

Table 4: The behavior of $\chi_2^{LO}, \Theta_2^{LO}$ on $\mathcal{R}^c(h)$ at large h and the number of oscillations, $N_{osc}^i(h)$, of $\{\chi_i^{LO}\}$ in the family of iso-energy return maps to Σ_i for sufficiently large h .

□

Table 5 displays the edge values at energies near h^{step} (i.e. for $h = h^{step} + \eta$, and small η). Notice that for such h values $\theta_i^*(h) = \sqrt{\eta/h_i^{step}}$ if $q_i^{wall} > 0$ and $\theta_i^*(h) = \pi - \sqrt{\eta/h_i^{step}}$ if $q_i^{wall} < 0$. We see that when $q_2^{wall} > 0$, infinite number of oscillations occur for arbitrary small η , whereas in the other cases, the number of oscillations scales with $\sqrt{\eta}$.

Corner position	χ_2^{LO}	Θ_2^{LO}	$N_{osc}^2(h^{step} + \eta)$
$q_{1,2}^{wall} < 0$	$0 \nearrow \searrow \frac{\omega_2}{\pi\omega_1} \sqrt{\frac{\eta}{h_1^{step}}}$	$2\pi \frac{\omega_2}{\omega_1} \searrow 2\frac{\omega_2}{\omega_1}(\pi - \sqrt{\eta/h_1^{step}})$	$\gtrsim \left\lfloor \frac{\omega_2}{\pi\omega_1} \sqrt{\frac{\eta}{h_1^{step}}} \right\rfloor$
$q_1^{wall} < 0, q_2^{wall} > 0$	$0 \nearrow \infty$	$2\pi \frac{\omega_2}{\omega_1} \searrow 2\frac{\omega_2}{\omega_1}(\pi - \sqrt{\eta/h_1^{step}})$	∞
$q_1^{wall} > 0, q_2^{wall} < 0$	$\frac{\omega_2}{\omega_1} + \frac{\omega_2}{\pi\omega_1} \sqrt{\frac{\eta}{h_2^{step}}} \searrow \frac{\omega_2}{\omega_1} - \frac{\omega_2}{\pi\omega_1} \sqrt{\frac{\eta}{h_1^{step}}}$	$0 \nearrow \sqrt{\eta/h_1^{step}}$	$\left\lfloor \frac{\omega_2}{\pi\omega_1} \sqrt{\frac{\eta}{h_1^{step}}} (1 + \sqrt{\frac{h_1^{step}}{h_2^{step}}}) \right\rfloor$
$q_{1,2}^{wall} > 0$	$\frac{\pi\omega_2}{\omega_1} \sqrt{\frac{h_2^{step}}{\eta}} \searrow \nearrow \infty$	$0 \nearrow \sqrt{\eta/h_1^{step}}$	∞

Table 5: The values of $\chi_2^{LO}, \Theta_2^{LO}$ at the edges of $\mathcal{R}^c(h = h^{step} + \eta)$ for small η , namely $\chi_2^{LO}(h_1^{step}), \chi_2^{LO}(\eta + h^{step} - h_2^{step})$ and $N_{osc}^2(h)$. The values of $N_{osc}^1(h)$ in the first and second rows are found by switching $1 \leftrightarrow 2$ (as in Table 4).

7 Summary and discussion

An integrable mechanical Hamiltonian system with a step barrier in the configuration space which is aligned with the continuous symmetries of the integrable Hamiltonian produces dynamics that are not Liouville integrable, yet are analyzable. An experimental setup which realizes such a theoretical model has been suggested (Fig 1). In such models, the motion on energy surfaces is foliated by level sets, yet, the motion on a range of iso-energy level sets is non-integrable and is conjugated to the motion on a family of genus 2 flat surfaces or, equivalently, to an L-shaped billiard (Theorem 2.1). The return map to a Poincaré section for this range of level sets is a 5 interval exchange map, and the lengths of the intervals change non-trivially along iso-energy family of level sets (Theorem 4.2). For the case of Linear oscillators the L-shaped billiard dimensions and thus the intervals lengths are found explicitly (Theorem 2.5) whereas for general non-linear oscillators they are given up to quadratures. While our main example included a single step, the same strategy may be applied to any barrier geometry which combines horizontal and vertical barriers. The flow of the HIS (1) with such barriers is conjugated, for any given level set, to a directional motion in the angles' space on nibbled rectangles with rectangular holes as analyzed in [10]. An important conclusion is that above certain energy the energy surfaces of (1) are foliated by several families of level set surfaces; within any such family the geometry varies smoothly, and different families have distinct topology. Namely, on the same energy surface there are families of level-set surfaces with different number of connected components and different numbers of holes (see corollary 2.2 and Fig. 10).

The implications of our findings are intriguing; First, the statistics of a typical observable of such mechanical systems (i.e. an observable which does not depend only on the energy distribution among the d.o.f.) are now related to the delicate theories derived for studying IEM and Teichmüller flows on moduli spaces. Second, by considering soft steep potentials instead of impacts, the

topology of the energy surfaces remains as complex as the one constructed here (then the motion is not expected to be foliated to level sets). Higher dimensional extensions, other symmetries, potentials with local maxima (so that the smooth system has singular level sets of the Liouville foliation), and the influence of small perturbations and soft potentials are exciting directions to be further explored (see related results in [19, 16]).

Acknowledgments

Supported by ISF 1208/16 and partially by the National Science Foundation under Grant No. 1440140, while one of the authors (VRK) was in residence at the Mathematical Sciences Research Institute in Berkeley, California, during the Fall semester of 2018. LB, SE, BF and SGC visit and work was supported by the Bessie Laurence International Summer Science Institute at the Weizmann institute. VRK thanks K. Frączek and B. Weiss for their valuable explanations on the dynamics on families of flat surfaces.

References

- [1] ARNOLD, V., KOZLOV, V., AND NEISHTADT, A. *Mathematical Aspects of Classical and Celestial Mechanics*, vol. 3. Springer Science & Business Media, 2007.
- [2] ATHREYA, J. S., ESKIN, A., AND ZORICH, A. Right-angled billiards and volumes of moduli spaces of quadratic differentials on $\mathbb{C}P^1$.
- [3] CHENG, J., AND WOJTKOWSKI, M. P. Linear stability of a periodic orbit in the system of falling balls. In *The geometry of Hamiltonian systems (Berkeley, CA, 1989)*, vol. 22 of *Math. Sci. Res. Inst. Publ.* Springer, New York, 1991, pp. 53–71.
- [4] DEMARCO, L. The conformal geometry of billiards. *Bulletin of the American Mathematical Society* 48, 1 (2011), 33–52.
- [5] DRAGOVIĆ, V., AND RADNOVIĆ, M. *Poncelet porisms and beyond*. Frontiers in Mathematics. Birkhäuser/Springer Basel AG, Basel, 2011. Integrable billiards, hyperelliptic Jacobians and pencils of quadrics.
- [6] DRAGOVIĆ, V., AND RADNOVIĆ, M. Pseudo-integrable billiards and arithmetic dynamics. *Journal of Modern Dynamics* 8, 1 (jul 2014), 109–132.
- [7] DRAGOVIĆ, V., AND RADNOVIĆ, M. Periods of pseudo-integrable billiards. *Arnold Mathematical Journal* 1, 1 (jan 2015), 69–73.

- [8] DULLIN, H. Linear stability in billiards with potential. *Nonlinearity* 11, 1 (1998), 151.
- [9] FEDOROV, Y. N. An ellipsoidal billiard with a quadratic potential. *Funktsional. Anal. i Prilozhen.*, 35, 3 (2001), 48–59.
- [10] FRĄCZEK, K. Recurrence for smooth curves in the moduli space and application to the billiard flow on nibbled ellipses. *arXiv preprint arXiv:1904.12715* (2019).
- [11] FRĄCZEK, K., SHI, R., AND ULCIGRAI, C. Genericity on curves and applications: pseudo-integrable billiards, eaton lenses and gap distributions. *Journal of Modern Dynamics* 12, 1 (2018), 55–122.
- [12] GORELYSHEV, I., AND NEISHTADT, A. On the adiabatic perturbation theory for systems with impacts. *Journal of applied mathematics and mechanics* 70, 1 (2006), 4–17.
- [13] GORELYSHEV, I., AND NEISHTADT, A. Jump in adiabatic invariant at a transition between modes of motion for systems with impacts. *Nonlinearity* 21, 4 (2008), 661.
- [14] KIM, D. H., MARCHESE, L., AND MARMI, S. Long hitting time for translation flows and l-shaped billiards. *arXiv preprint arXiv:1705.03328* (2017).
- [15] KLOC, M., AND ROM-KEDAR, V. Smooth Hamiltonian systems with soft impacts. *SIAM J. Appl. Dyn. Syst.* 13, 3 (2014), 1033–1059.
- [16] KLOC, M., AND ROM-KEDAR, V. Smooth Hamiltonian systems with soft impacts. *SIAM Journal on Applied Dynamical Systems* 13, 3 (2014), 1033–1059.
- [17] KOZLOV, V., AND TRESHCHĖV, D. *Billiards: a genetic introduction to the dynamics of systems with impacts*, vol. 89. American Mathematical Soc., 1991.
- [18] LERMAN, L., AND ROM-KEDAR, V. A saddle in a corner—a model of collinear triatomic chemical reactions. *SIAM J. Appl. Dyn. Syst.* 11, 1 (2012), 416–446.
- [19] PNUELI, M., AND ROM-KEDAR, V. On near integrability of some impact systems. *SIAM J. Appl. Dyn. Syst.* 17, 4 (2018), 2707 – 2732.
- [20] PNUELI, M., AND ROM-KEDAR, V. On the structure of hamiltonian impact systems. *arXiv preprint arXiv:1903.08851* (2019).
- [21] RADNOVIC, M. Topology of the elliptical billiard with the hooke’s potential. *Theoretical and Applied Mechanics* 42, 1 (2015), 1–9.

- [22] STURMAN, R. The role of discontinuities in mixing. In *Advances in applied mechanics*, vol. 45. Elsevier, 2012, pp. 51–90.
- [23] VEECH, W. A. Gauss measures for transformations on the space of interval exchange maps. *Annals of Mathematics* 115, 2 (1982), 201–242.
- [24] WOJTKOWSKI, M. P. Complete hyperbolicity in Hamiltonian systems with linear potential and elastic collisions. In *Proceedings of the XXX Symposium on Mathematical Physics (Toruń, 1998)* (1999), vol. 44, pp. 301–312.
- [25] ZHARNITSKY, V. Invariant tori in Hamiltonian systems with impacts. *Communications in Mathematical Physics* 211, 2 (2000), 289–302.
- [26] ZORICH, A. Square tiled surfaces and teichmüller volumes of the moduli spaces of abelian differentials. In *Rigidity in dynamics and geometry*. Springer, 2002, pp. 459–471.
- [27] ZORICH, A. Flat surfaces. *Frontiers in number theory, physics, and geometry I* (2006), 439–585.